



Principal-component analysis of two-particle azimuthal correlations in PbPb and pPb collisions at CMS

The CMS Collaboration*

Abstract

For the first time a principle-component analysis is used to separate out different orthogonal modes of the two-particle correlation matrix from heavy ion collisions. The analysis uses data from $\sqrt{s_{\text{NN}}} = 2.76$ TeV PbPb and $\sqrt{s_{\text{NN}}} = 5.02$ TeV pPb collisions collected by the CMS experiment at the LHC. Two-particle azimuthal correlations have been extensively used to study hydrodynamic flow in heavy ion collisions. Recently it has been shown that the expected factorization of two-particle results into a product of the constituent single-particle anisotropies is broken. The new information provided by these modes may shed light on the breakdown of flow factorization in heavy ion collisions. The first two modes (“leading” and “subleading”) of two-particle correlations are presented for elliptical and triangular anisotropies in PbPb and pPb collisions as a function of p_T over a wide range of event activity. The leading mode is found to be essentially equivalent to the anisotropy harmonic previously extracted from two-particle correlation methods. The subleading mode represents a new experimental observable and is shown to account for a large fraction of the factorization breaking recently observed at high transverse momentum. The principle-component analysis technique has also been applied to multiplicity fluctuations. These also show a subleading mode. The connection of these new results to previous studies of factorization is discussed.

Published in Physical Review C as doi:10.1103/PhysRevC.96.064902.

1 Introduction

The primary goal of experiments with heavy ion collisions at ultra-relativistic energies is to study nuclear matter under extreme conditions. Quantum chromodynamics on the lattice predicts the formation of a quark-gluon plasma (QGP) at energies densities that are attainable in relativistic heavy ion collisions. Measurements carried out at the Relativistic Heavy Ion Collider (RHIC) indicate that a strongly interacting QGP is produced in heavy ion collisions [1–4]. The presence of azimuthal anisotropy in the emission of final state hadrons revealed a strong collective flow behavior of this strongly coupled hot and dense medium [5, 6]. The significantly higher energies available at the CERN LHC compared to RHIC have allowed the ALICE, ATLAS, and CMS experiments to make very detailed measurements of the QGP properties [7–15]. The collective expansion of the QGP can be described by hydrodynamic flow models [16–18]. In the context of these models, the azimuthal anisotropy of hadron emission is the response to the initial density profile of the overlap region of the colliding nuclei. Such anisotropic emission, for a given event, can be quantified through a Fourier decomposition of the single-particle distribution

$$\frac{dN}{d\mathbf{p}} = \sum_{n=-\infty}^{\infty} V_n(p) e^{-in\phi}, \quad (1)$$

with $V_n(p) = v_n(p) e^{in\Psi_n(p)}$, $d\mathbf{p} = dp_T d\phi d\eta$, and p being a shorthand notation for p_T and η . This single-particle distribution is the invariant yield of emitted particles N expressed in phase space p_T , η and ϕ , i.e., transverse momentum, pseudorapidity, and azimuthal angle. Here, v_n corresponds to the real single-particle anisotropy and $\Psi_n(p)$ represents the n th order event plane angle. Also, because of the reflection symmetry of the overlap region, the relation $V_n^* = V_{-n}$ holds for the complex harmonics. Using this relation and integrating Eq. (1) over a given pseudorapidity and p_T window yields

$$\frac{dN}{d\phi} = \frac{N}{2\pi} \left(1 + 2 \sum_{n=1}^{\infty} v_n(p) \cos[n(\phi - \Psi_n(p))] \right). \quad (2)$$

Note that the single-particle anisotropy coefficient v_n is generally a function of p_T and η , which is also the case for the event plane angle. The azimuthal correlation of N^{pairs} emitted particle pairs (with particles labeled a and b) as a function of their azimuthal separation $\Delta\phi^{ab} = \phi^a - \phi^b$ can be characterized by its own Fourier harmonics

$$\frac{dN^{\text{pairs}}}{d\Delta\phi^{ab}} = \frac{N^{\text{pairs}}}{2\pi} \left(1 + 2 \sum_{n=1}^{\infty} V_{n\Delta}(p^a, p^b) \cos(n\Delta\phi) \right), \quad (3)$$

where $V_{n\Delta}$ is the two-particle harmonic. In a pure hydrodynamic picture, as a consequence of independent particle emission, the flow hypothesis connects the single- and two-particle spatial anisotropies from Eqs. (2) and (3) through factorization. In other words, particles carry information only about their orientation with respect to the whole system and the two-particle distribution can therefore be factorized based on

$$\left\langle \frac{dN^{\text{pairs}}}{d\Delta\phi^{ab}} \right\rangle = \left\langle \frac{dN}{d\phi^a} \frac{dN}{d\phi^b} \right\rangle, \quad (4)$$

with the bracket $\langle \rangle$ representing the average over all events of interest. This equality can be investigated by looking at the connection between the single- and two-particle harmonics

$$\langle V_{n\Delta}(p^a, p^b) \rangle = \langle V_n(p^a) V_n^*(p^b) \rangle = \langle v_n^a v_n^b \cos[n(\Psi_n^a - \Psi_n^b)] \rangle \leq \langle v_n^a v_n^b \rangle. \quad (5)$$

From Eq. (5) we infer that factorization is preserved when the cosine value equals unity. This scenario is possible only when the event plane angle acts as a global phase, lacking any p_T or η dependence for a given event. Thus, measurements of the momentum space fluctuations (correlations) constrain the initial state and properties of QGP expansion dynamics. Previous measurements have shown a significant breakdown of factorization at high p_T in ultracentral (i.e., almost head-on) PbPb collisions [15]. A smaller effect was also seen in high-multiplicity pPb collisions [19]. Furthermore, significant factorization breakdown effects as a function of η were observed in both PbPb and high-multiplicity pPb collisions [19]. Several possible explanations for the observed factorization breaking have been proposed. One expected contribution arises from nonflow effects, i.e. short-range correlations mainly due to jet fragmentation and resonance decays. However, factorization breaking is also possible in hydrodynamic models, once the effects of event-by-event initial-state fluctuations are taken into account [20, 21]. Such a nonuniform initial-state energy density can arise from fluctuations in the positions of nucleons within nuclei and/or the positions of quark and gluon constituents inside each nucleon, giving rise to variations in the collision points when the two nuclei collide. The resulting fluctuating initial energy density profile creates nonuniformities in pressure gradients which push particles in different regions of phase space in directions that vary randomly about a mean angle, thereby imprinting these fluctuations on the final particle distributions. Consequently, the event plane angles estimated from particles in different p_T and η ranges may vary with respect to each other. By introducing such a dependence, $\Psi_n = \Psi_n(p_T, \eta)$, it is possible to describe the resulting final-state particle distributions using hydrodynamical models [20, 21].

Principal-component analysis (PCA) is a multivariate technique that can separate out the different orthogonal contributions (also known as modes) to the fluctuations. Using the method introduced in Ref. [22], this paper presents the first experimental use of applying PCA to two-particle correlations in order to study factorization breaking as a function of p_T . This allows the extraction of a new experimental observable, the subleading mode, which is directly connected to initial-state fluctuations and their effect on factorization breaking.

2 Experimental setup and data samples

The Compact Muon Solenoid (CMS) is an axially symmetric detector with an onion-like structure, which consists of several subsystems concentrically placed around the interaction point. The CMS magnet is a superconducting solenoid providing a magnetic field of 3.8 T, which allows precise measurement of charged particle momentum. The muon chambers are placed outside the solenoid. In this analysis the data used is extracted from the silicon tracker, which is the closest subdetector to the interaction point. This detector consists of 1440 silicon pixel and 15 148 silicon strip detector modules that detect hit locations, from which the charged particle trajectories are reconstructed. The silicon tracker covers charged particles within the range $|\eta| < 2.5$, and provides an impact parameter resolution of $\sim 15 \mu\text{m}$ and a p_T resolution better than 1.5% up to $p_T \sim 100 \text{ GeV}/c$.

The other two subdetectors located inside the solenoid, are the electromagnetic calorimeter (ECAL) and hadronic calorimeter (HCAL). The ECAL is constructed of 75 848 lead-tungstate crystals which are arranged in a quasi-projective geometry and cover a pseudorapidity range of $|\eta| < 1.48$ units in the barrel and two endcaps that extend $|\eta|$ up to 3.0. The HCAL barrel and endcaps are sampling calorimeters constructed from brass and scintillator plates, covering $|\eta| < 3.0$. Additional extension in $|\eta|$ from 2.9 up to 5.2 is achieved with the iron and quartz-fiber Čerenkov Hadron Forward (HF) calorimeters on either side of the interaction region. The HF calorimeters are segmented into towers, each of which is a two-dimensional cell with a

granularity of $0.175 \times 0.175 \text{ rad}^2$ ($\Delta\eta \times \Delta\phi$). The zero-degree calorimeters (ZDC) are tungsten-quartz Cherenkov calorimeters located at $\pm 140 \text{ mm}$ from the interaction point [23]. They are designed to measure the energy of photons and spectator neutrons emitted from heavy ion collisions. A set of scintillator tiles, the beam scintillator counters (BSC), are mounted on the inner side of the HF calorimeters and are used for triggering and beam-halo rejection. The BSCs cover the range $3.23 < |\eta| < 4.65$. A detailed description of the CMS detector can be found in Ref. [24].

This analysis is performed using data recorded by the CMS experiment during the LHC heavy ion runs in 2011 and 2013. The PbPb data set at a center-of-mass energy of $\sqrt{s_{\text{NN}}} = 2.76 \text{ TeV}$ corresponds to an integrated luminosity of about $159 \mu\text{b}^{-1}$, while the pPb data set at $\sqrt{s_{\text{NN}}} = 5.02 \text{ TeV}$ corresponds to about 35 nb^{-1} . During the pPb run, the beam energies were 4 TeV for protons and 1.58 TeV per nucleon for lead nuclei.

3 Selection of events and tracks

Online triggers, track reconstruction, and offline event selections are the same as in Refs. [15, 19, 25] for PbPb and pPb data samples, and are summarized in the following sections.

3.1 The PbPb data

Minimum bias PbPb events were collected using coincident trigger signals from both ends of the detector in either BSCs or the HF calorimeters. Events affected by cosmic rays, detector noise, out-of-time triggers, and beam backgrounds were suppressed by requiring a coincidence of the minimum bias trigger with bunches colliding in the interaction region. The efficiency of the trigger is more than 97% in case of hadronic inelastic PbPb collisions. Because of hardware limits on the data acquisition rate, only a small fraction (2%) of all minimum bias events were recorded (i.e., the trigger is “prescaled”). To enhance the event sample for very central PbPb collisions, a dedicated online trigger was implemented by simultaneously requiring the HF transverse energy (E_T) sum to be greater than 3260 GeV and the pixel cluster multiplicity to be greater than 51400 (which approximately corresponds to 9500 charged particles over 5 units of η). The selected events correspond to the 0–0.2% most central PbPb collisions. Other standard PbPb centrality classes presented in this paper were determined based on the total energy deposited in the HF calorimeters [13]. The inefficiencies of the minimum bias trigger and event selection for very peripheral events are taken into account.

In order to reduce further the background from single-beam interactions (e.g., beam gas and beam halo), cosmic muons, and ultraperipheral collisions leading to the electromagnetic breakup of one or both Pb nuclei [26], offline PbPb event selection criteria [13] were applied by requiring energy deposits in at least three towers in each of the HF calorimeters, with at least 3 GeV of energy in each tower, and the presence of a reconstructed primary vertex built of at least two tracks. The reconstructed primary vertex is required to be located within $\pm 15 \text{ cm}$ of the average interaction point along the beam axis and within a radius of 0.2 cm in the transverse plane. Following the procedure developed in Ref. [15], events with large signals in both ZDCs and HFs are identified as having at least one additional interaction, or pileup events, and are thus rejected (about 0.1% of all events).

The reconstruction of the primary event vertex and of the trajectories of charged particles in PbPb collisions is based on signals in the silicon pixel and strip detectors and is described in detail in Ref. [13]. From studies based on PbPb events simulated using HYDJET v1.8 [27], the combined geometrical acceptance and reconstruction efficiency of the primary tracks is about

70% at $p_T \sim 1 \text{ GeV}/c$ and $|\eta| < 1.0$ for the most central (0–5%) PbPb events, but drops to about 50% for $p_T \sim 0.3 \text{ GeV}/c$. The fraction of misidentified tracks is kept to be $< 5\%$ over most of the p_T ($> 0.5 \text{ GeV}/c$) and $|\eta|$ (< 1.6) ranges. It increases to about 20% for very low p_T ($< 0.5 \text{ GeV}/c$) particles in the forward ($|\eta| \geq 2.0$) region.

3.2 The pPb data

Minimum bias pPb events were triggered by requiring at least one track with $p_T > 0.4 \text{ GeV}/c$ to be found in the pixel tracker in coincidence with an LHC pPb bunch crossing. From all minimum bias triggered events, only a fraction of ($\sim 10^{-3}$) was recorded. In order to select high-multiplicity pPb collisions, a dedicated trigger was implemented using the CMS level-1 (L1) and high-level trigger (HLT) systems. At L1, the total transverse energy summed over the ECAL and HCAL is required to be greater than a given threshold (20 or 40 GeV). The online track reconstruction for the HLT is based on the three layers of pixel detectors, and requires a track originated within a cylindrical region of length 30 cm along the beam and radius of 0.2 cm perpendicular to the beam. For each event, the vertex reconstructed with the highest number of pixel tracks is selected. The number of pixel tracks ($N_{\text{tk}}^{\text{online}}$) with $|\eta| < 2.4$, $p_T > 0.4 \text{ GeV}/c$, and having a distance of closest approach of 0.4 cm or less to this vertex, is determined for each event.

In the offline analysis, hadronic pPb collisions are selected by requiring a coincidence of at least one HF calorimeter tower with more than 3 GeV of total energy in each of the HF detectors. Events are also required to contain at least one reconstructed primary vertex within 15 cm of the nominal interaction point along the beam axis and within 0.15 cm transverse to the beam trajectory. At least two reconstructed tracks are required to be associated with the primary vertex. Beam-related background is suppressed by rejecting events for which less than 25% of all reconstructed tracks are of good quality (i.e., the tracks selected for physics analysis).

The instantaneous luminosity provided by the LHC in the 2013 pPb run resulted in approximately 3% probability of at least one additional interaction occurring in the same bunch crossing, i.e. pileup events. Pileup was rejected using a procedure based on the number of tracks in a given vertex and the distance between that an additional vertex (see Ref. [25]). The fraction of pPb events selected by these criteria, which have at least one particle (proper lifetime $\tau > 10^{-18} \text{ s}$) with total energy $E > 3 \text{ GeV}$ in η range of $-5 < \eta < -3$ and at least one in the range $3 < \eta < 5$ (selection referred to as “double-sided”) has been found to be 97–98% by using the EPOS [28] and HIJING [29] event generators.

In this analysis, the CMS highPurity [30] tracks are used. Additionally, a reconstructed track is only considered as a primary-track candidate if the significance of the separation along the beam axis (z) between the track and the best vertex, $dz/\sigma(dz)$, and the significance of the impact parameter relative to the best vertex transverse to the beam, $d_T/\sigma(d_T)$, are less than 3 in each case. The relative uncertainty of the p_T measurement, $\sigma(p_T)/p_T$, is required to be less than 10%. To ensure high tracking efficiency and to reduce the rate of misidentified tracks, only tracks within $|\eta| < 2.4$ and with $p_T > 0.3 \text{ GeV}/c$ are used in the analysis. The entire pPb data set is divided into classes of reconstructed track multiplicity, $N_{\text{tk}}^{\text{offline}}$, where primary tracks with $|\eta| < 2.4$ and $p_T > 0.4 \text{ GeV}/c$ are counted. The multiplicity classification in this analysis is identical to that used in Ref. [25], where more details are provided.

4 Analysis technique

This analysis uses two-particle correlations and PCA as a new flow method that can make use of all the information contained in $V_{n\Delta}$ harmonics. Averaging Eq. (3) over all events of interest, within a given reference bin p_T^{ref} , and assuming factorization, one can write

$$\left\langle \frac{dN^{\text{pairs}}}{d\Delta\phi} \right\rangle = \frac{\langle N^{\text{pairs}} \rangle}{2\pi} \left(1 + \sum_{n=1}^{\infty} v_n^2\{2\} \cos(n\Delta\phi) \right), \quad (6)$$

where $v_n\{2\}$ is the integrated reference flow calculated from the $V_{n\Delta}$ as

$$v_n\{2\} = \frac{\sqrt{V_{n\Delta}(p_T^{\text{ref}}, p_T^{\text{ref}})}}{\sqrt{V_{0\Delta}(p_T^{\text{ref}}, p_T^{\text{ref}})}}, \quad (7)$$

with,

$$V_{n\Delta}(p_T^{\text{ref}}, p_T^{\text{ref}}) \equiv \left\langle \sum_{i \in \text{ref}} \cos(n\Delta\phi_i) \right\rangle. \quad (8)$$

Here, the label $V_{0\Delta}$ for N^{pairs} is used, since the sum over cosine counts the number of pairs for the $n = 0$ case. Calculating the differential flow one gets

$$v_n(p_T)\{2\}v_n\{2\} = \frac{V_{n\Delta}(p_T, p_T^{\text{ref}})}{V_{0\Delta}(p_T, p_T^{\text{ref}})}, \quad (9)$$

or,

$$v_n(p_T) = \frac{V_{n\Delta}(p_T, p_T^{\text{ref}})}{\sqrt{V_{n\Delta}(p_T^{\text{ref}}, p_T^{\text{ref}})}} \frac{\sqrt{V_{0\Delta}(p_T^{\text{ref}}, p_T^{\text{ref}})}}{V_{0\Delta}(p_T, p_T^{\text{ref}})}. \quad (10)$$

The single-particle anisotropy definition in Eq. (10) includes the $V_{0\Delta}$ terms to compensate for the fact that the $V_{n\Delta}$ Fourier harmonics are calculated without per-event normalization by the number of pairs in the given bin [15, 19]. This way of calculating the cosine term is essential for the PCA to work, since it gives a weight to a bin that is of the order of the number of particles in it [22].

In a realistic experiment, the $V_{n\Delta}$ harmonics of Eq. (8) are affected by imperfections in the detector and take the following operational definition

$$V_{n\Delta}(p_T^a, p_T^b) = \langle \cos(n\Delta\phi) \rangle_S - \langle \cos(n\Delta\phi) \rangle_B, \quad n = 1, 2, 3, \dots \quad (11)$$

Here, the first term in the right-hand side of Eq. (11), $\langle \cos(n\Delta\phi) \rangle_S$, is the two-particle anisotropic signal where the correlated particles belong to the same event. The second term, $\langle \cos(n\Delta\phi) \rangle_B$ is a background term that accounts for the nonuniform acceptance of the detector. This term is usually two orders of magnitude smaller than the corresponding signal. It is estimated by mixing particle tracks from two random events. These two events have the same 2 cm wide range of the primary vertex position in the z direction and belong to the same centrality (track multiplicity) class. For both terms, in order to suppress nonflow correlations, a pseudorapidity difference requirement between the two tracks $|\Delta\eta| > 2$ is applied.

4.1 Factorization breaking

The PCA is a multivariate analysis that orders the fluctuations in the data by size. The ordering is done through principal components that represent orthogonal eigenvectors of the corresponding covariance data matrix. In the context of flow fluctuations, the components should reveal any significant substructure caused by the fluctuating initial state geometry of colliding nuclei. Introducing PCA in terms of factorization breaking one can write the Pearson correlation coefficient used for measurement of the effect as in Ref. [19]

$$r_n(p_T^a, p_T^b) \equiv \frac{V_{n\Delta}(p_T^a, p_T^b)}{\sqrt{V_{n\Delta}(p_T^a, p_T^a)V_{n\Delta}(p_T^b, p_T^b)}} \approx \langle \cos n(\Psi(p_T^a) - \Psi(p_T^b)) \rangle. \quad (12)$$

The ratio r_n is approximated by the cosine term, giving unity if the event plane angle is a global phase, as discussed previously. Expressing the ratio through the two-particle harmonic in complex form from Eq. (5), r_n can only be unity if the complex flow coefficient $V_n(p_T)$ is generated from one initial geometry. For instance, where the initial geometry of the overlap region is defined by some complex eccentricity (ε_n) and a fixed real function $f(p_T)$, i.e., $V_n(p_T) = f(p_T)\varepsilon_n$. However, if events are described by multiple eccentricities then r_n may be less than unity and the flow pattern displays factorization breaking [31]. This last statement can be generalized by expanding the complex flow coefficient using the principal components ($V_n^{(1)}(p_T), V_n^{(2)}(p_T), \dots$) as a basis built from a covariance data matrix of given size $N_\alpha \times N_\alpha$

$$V_n(p_T) = \zeta_n^{(1)} V_n^{(1)}(p_T) + \zeta_n^{(2)} V_n^{(2)}(p_T) + \dots + \zeta_n^{(N_\alpha)} V_n^{(N_\alpha)}(p_T), \quad (13)$$

where $\zeta_n^{(i)}$ are complex uncorrelated variables with zero mean i.e. $\langle \zeta_n^{(i)} \zeta_n^{(j)} \rangle = \delta_{ij}$, $\langle \zeta_n^{(i)} \rangle = 0$, and N_α represents the number of p_T differential bins. Therefore, the two-particle harmonics are the building elements of the covariance data matrix $[\hat{V}_{n\Delta}(p_T^a, p_T^b)]_{N_\alpha \times N_\alpha}$.

A covariance matrix is symmetrical and positive semidefinite (i.e., with eigenvalues $\lambda \geq 0$). For the flow matrix, the last trait is valid if there are no nonflow contributions and no strong statistical fluctuations [22]. Now, calculating the two-particle harmonic using the expansion from Eq. (13) one gets

$$V_{n\Delta}(p_T^a, p_T^a) = \sum_{\alpha=1}^{N_\alpha} V_n^{(\alpha)}(p_T^a) V_n^{(\alpha)}(p_T^a). \quad (14)$$

Here, the principal components will be referred to as modes [22, 31, 32]. In order to calculate the modes the spectral decomposition is rewritten as:

$$V_{n\Delta}(p_T^a, p_T^b) = \sum_{\alpha} \lambda^{(\alpha)} e^{(\alpha)}(p_T^a) e^{(\alpha)}(p_T^b), \quad (15)$$

which gives:

$$V_n^{(\alpha)}(p_T) = \sqrt{\lambda^{(\alpha)}} e^{(\alpha)}(p_T), \quad (16)$$

where $e^{(\alpha)}(p_T)$ are (α) index values of normalized eigenvectors and $\lambda^{(\alpha)}$ eigenvalues that are sorted in a strict decreasing order $\lambda^{(1)} > \lambda^{(2)} > \dots > \lambda^{(n)}$. Eq. (14) shows directly that factorization holds only in the case where just one mode is present. If multiple modes are present in the data, Eqs. (15) and (16) allow to define a normalized orthogonal basis for the total v_n given in Eq. (10). These basis vectors are defined by:

$$v_n^{(\alpha)}(p_T) \equiv \frac{V_n^{(\alpha)}(p_T)}{V_0^{(1)}(p_T)}. \quad (17)$$

The normalization factor $V_0^{(1)}$ is the first mode that would follow from Eq. (16) using the matrix of the number of pairs, i.e., the matrix of $V_{0\Delta}$ terms. In practice, the mode $V_0^{(1)}$ has a simple physical meaning: it is the average differential multiplicity $\langle M(p_T) \rangle$. However, given the pseudorapidity requirement in the correlations, $V_0^{(1)}$ is proportional to $\langle \sqrt{N_{|\Delta\eta|>2}^{\text{pairs}}(p_T, p_T)} \rangle$. In order to restore normalization by the average bin multiplicity $\langle M(p_T) \rangle$ an intermediate step is made by multiplying the $V_{n\Delta}(p_T^a, p_T^b)$ with:

$$\zeta = \left\langle \frac{V_0^{|\eta|<2.4}(p_T^a, p_T^b)}{V_0^{|\Delta\eta|>2}(p_T^a, p_T^b)} \right\rangle, \quad (18)$$

ζ being the mean value of the ratio of number of all pairs and number of pairs after applying $|\Delta\eta| > 2$ selection for the given bins. If the η distribution of particles did not depend upon p_T then $\zeta(p_T^a, p_T^b)$ would be constant for all values of p_T^a and p_T^b . In fact, ζ does have a slight dependence on p_T^a and p_T^b with a maximum at low values of p_T^a and p_T^b . As events become more central the center of gravity of zeta moves to higher p_T values. Finally, after applying this correction the eigenvalue problem is solved with new matrix elements

$$\tilde{V}_{n\Delta}(p_T^a, p_T^b) \equiv \zeta V_{n\Delta}(p_T^a, p_T^b). \quad (19)$$

Eq. (17) then becomes:

$$v_n^{(\alpha)}(p_T) = \frac{\tilde{V}_n^{(\alpha)}(p_T)}{\langle M(p_T) \rangle}. \quad (20)$$

The leading ($\alpha = 1$) and the subleading ($\alpha = 2$) normalized modes (for simplicity, term modes will be used) can be thought of as new experimental observables. Given that the eigenvalues $\lambda^{(\alpha)}$ are strongly ordered, two components typically describe the variance in the harmonic flow to high accuracy. The leading mode is strongly correlated with the event plane, and thus is essentially equivalent to the standard definition of the single-particle anisotropic flow, while the subleading mode is uncorrelated with the event plane, and thus quantifies the magnitude of the factorization breaking caused by the initial-state fluctuations.

4.2 Multiplicity fluctuations

The PCA can also be applied for investigating multiplicity fluctuations in heavy ion collisions. The multiplicity matrix that is used for extraction of the corresponding modes is built from the following matrix elements:

$$[\hat{M}(p_T^a, p_T^b)]_{N_\alpha \times N_\alpha} = \langle V_{0\Delta}(p_T^a, p_T^b) \rangle - \langle M(p_T^a) \rangle \langle M(p_T^b) \rangle, \quad (21)$$

where the term $V_{0\Delta}(p_T^a, p_T^b)$ represents the number of pairs for the given bins and $M(p_T)$ the given bin multiplicity. Unlike in the flow cases $n = 2, 3$, here no pseudorapidity requirement $|\Delta\eta| > 2$ is applied when correlating tracks. Using the multiplicity matrix the modes defined by Eq. (16) are derived and the leading and subleading modes are calculated with Eq. (20), excluding the multiplication step in Eq. (19). The leading mode represents the “total multiplicity fluctuations”, i.e., if the higher modes are zero, then $v_0^{(1)}$ would approximately be equal to the standard deviation of multiplicity for the given p_T bin. The reconstructed subleading mode represents a new observable of the multiplicity spectrum. The multiplicity results in Section 6 represent exploratory studies and are for simplicity only presented for PbPb.

5 Systematic uncertainties

Several sources of possible systematic uncertainties, such as the event selection, the dimension of the matrix, and the effect of the tracking efficiency were investigated. Among these sources, only the effect of the tracking efficiency had a noticeable influence on the results. For all the considered cases $n = 0, 2, 3$ the systematic uncertainties were estimated from the full difference between the final result with and without the correction for the tracking efficiency. Each reconstructed track was weighted by the inverse of the efficiency factor, $\varepsilon_{\text{trk}}(p_T, \eta)$, which is a function of transverse momentum and pseudorapidity. The efficiency weighting factor accounts for the detector acceptance $A(p_T, \eta)$ and the reconstruction efficiency, $E(p_T, \eta)$ ($\varepsilon_{\text{trk}} = A E$).

From Eqs. (16) and (20) it can be seen that modes are functions of the eigenvectors and eigenvalues, i.e. e and λ , of the matrix, and of the differential multiplicity $M(p_T)$. When the efficiency correction is applied to each track, a completely new matrix is produced and the multiplicity of tracks also increases. The principal components of this new matrix were then calculated and new modes derived. This procedure gives a robust test of how susceptible the modes are to strong changes in (λ, e, M) . Table 1 summarizes the uncertainties of the subleading mode in the highest bin $2.5 < p_T < 3.0 \text{ GeV}/c$ for both the pPb and PbPb cases. The systematic uncertainties are estimated values and are rounded to the nearest integer. For the leading mode, systematic uncertainties are significant only for $n = 0$, while for the subleading mode systematic uncertainties are larger for all the cases $n = 0, 2, 3$. In the lower p_T range, for the multiplicity case $n=0$, the systematic uncertainties of the subleading mode are strongly correlated.

Table 1: Summary of estimated systematic uncertainties relative to the given mode for the last p_T bin $2.5 < p_T < 3.0 \text{ GeV}/c$ for PbPb and pPb data.

PbPb	$n = 2$		$n = 3$		$n = 0$	
Centrality (%)	$\alpha = 1$	$\alpha = 2$	$\alpha = 1$	$\alpha = 2$	$\alpha = 1$	$\alpha = 2$
0–0.2	1%	30%	1%	40%	40%	10%
0–5	1%	50%	1%	40%	15%	10%
0–10	1%	30%	1%	40%	10%	30%
10–20	1%	10%	1%	40%	10%	20%
20–30	1%	10%	1%	20%	10%	15%
30–40	1%	10%	1%	35%	10%	10%
40–50	1%	10%	1%	25%	10%	10%
50–60	1%	7%	1%	30%	10%	30%

pPb	$n = 2$		$n = 3$	
$N_{\text{trk}}^{\text{offline}}$	$\alpha = 1$	$\alpha = 2$	$\alpha = 1$	$\alpha = 2$
[220, 260)	1%	1.5%	1%	20%
[185, 220)	1%	2.0%	1%	20%
[150, 185)	1%	2.0%	1%	20%
[120, 150)	1%	2.0%	1%	20%

6 Results

Figure 1 shows leading and subleading modes for the elliptic case ($n = 2$) for eight centrality regions in PbPb collisions at $\sqrt{s_{\text{NN}}} = 2.76 \text{ TeV}$ as a function of p_T . These centrality regions range from ultracentral 0–0.2% to peripheral 50–60%. The data are binned into seven p_T bins covering the region $0.3 < p_T < 3.0 \text{ GeV}/c$. The number of differential p_T bins for constructing the covariance matrix is $N_\alpha = 7$. In all the figures the points are placed at the mean p_T

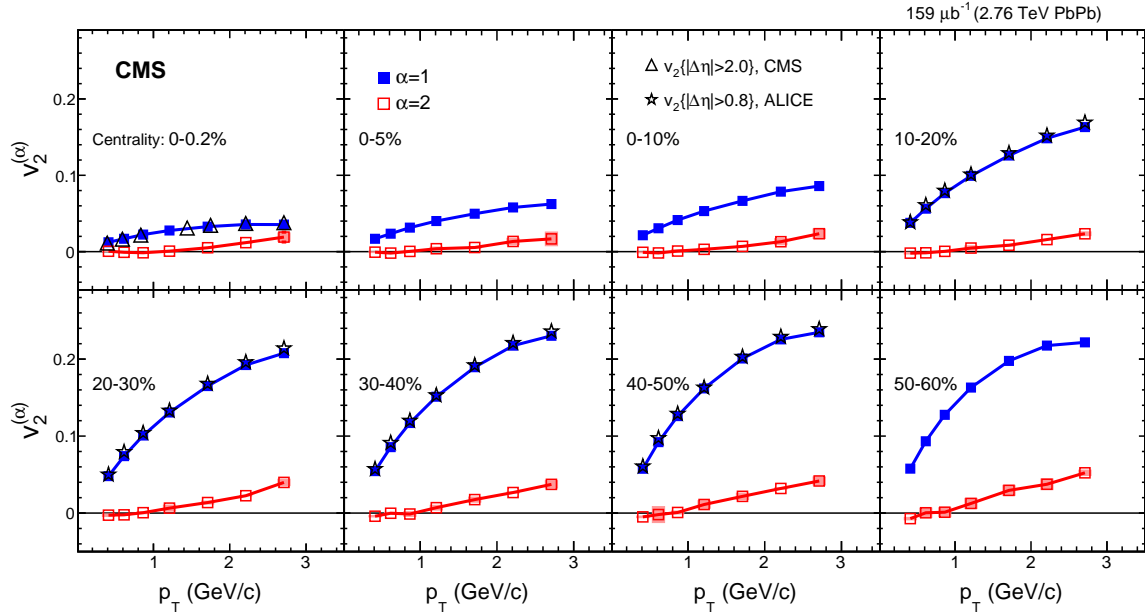


Figure 1: Leading ($\alpha = 1$) and subleading ($\alpha = 2$) modes for $n = 2$ as a function of p_T , measured in a wide centrality range of PbPb collisions at $\sqrt{s_{\text{NN}}} = 2.76$ TeV. The results for the leading mode ($\alpha = 1$) are compared to the standard elliptic flow magnitude measured by ALICE and CMS using the two-particle correlation method taken from Refs. [7, 15], respectively. The error bars correspond to statistical uncertainties and boxes to systematic ones.

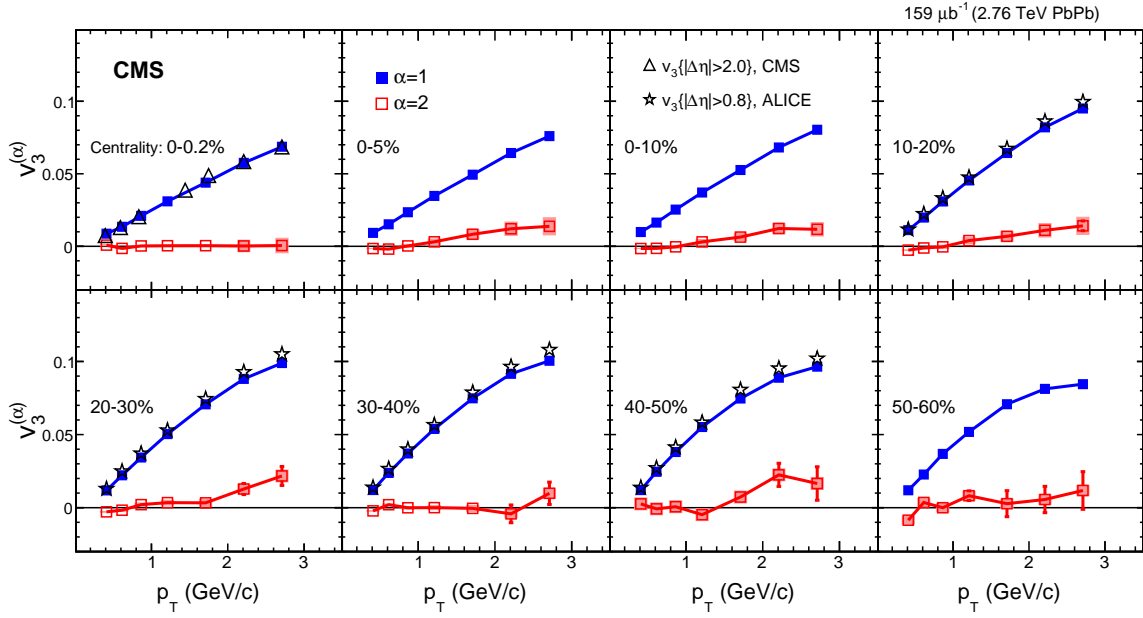


Figure 2: Leading ($\alpha = 1$) and subleading ($\alpha = 2$) modes for $n = 3$ as a function of p_T , measured in a wide centrality range of PbPb collisions at $\sqrt{s_{NN}} = 2.76$ TeV. The results for the leading mode ($\alpha = 1$) are compared to the standard triangular flow magnitude measured by ALICE and CMS using the two-particle correlation method taken from Refs. [7, 15], respectively. The error bars correspond to statistical uncertainties and boxes to systematic ones.

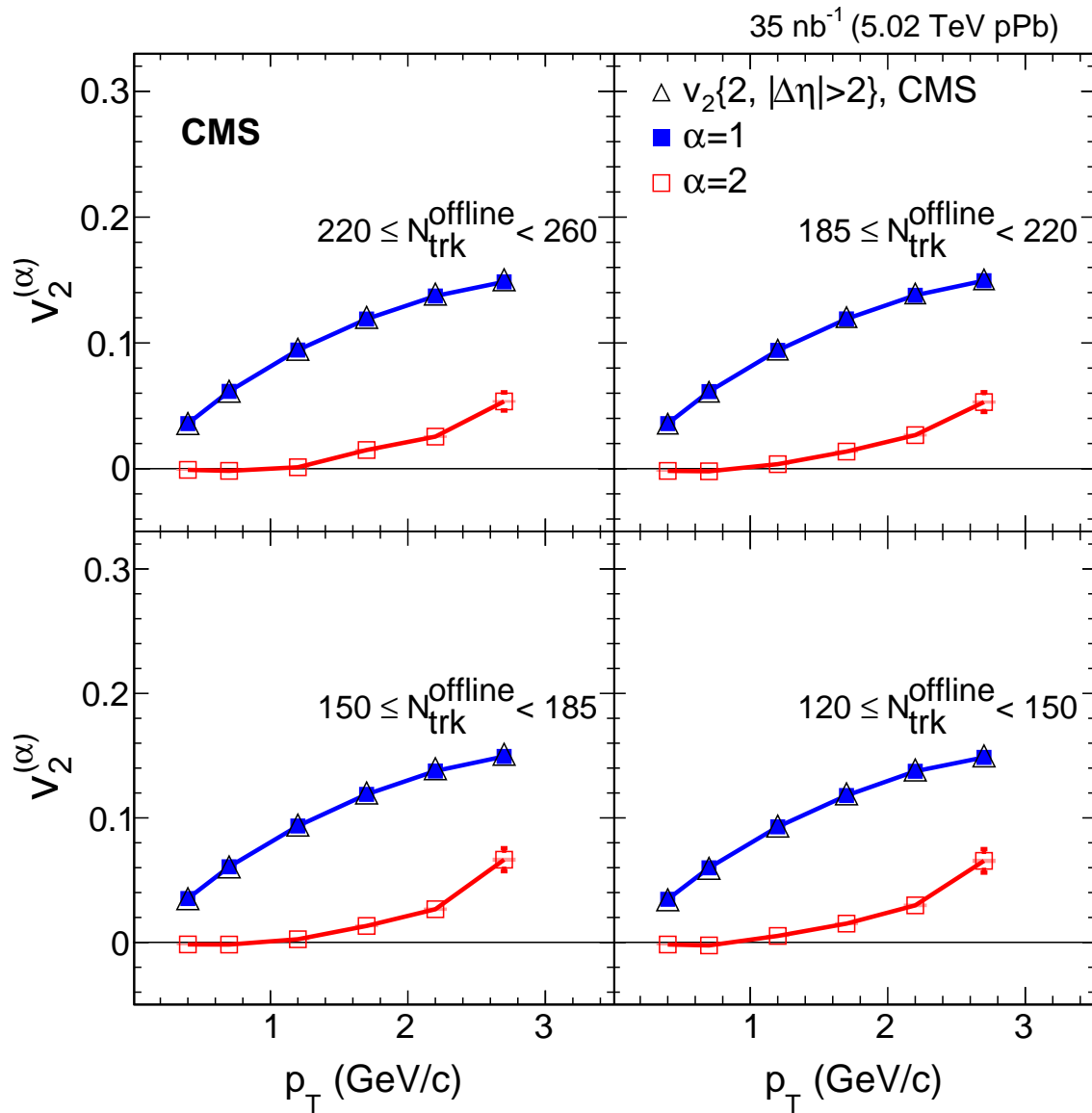


Figure 3: Leading ($\alpha = 1$) and subleading ($\alpha = 2$) modes for $n = 2$ as a function of p_T , measured in high-multiplicity pPb collisions at $\sqrt{s_{\text{NN}}} = 5.02$ TeV, for four classes of reconstructed track multiplicity $N_{\text{trk}}^{\text{offline}}$. The results for the leading mode ($\alpha = 1$) are compared to the standard elliptic flow magnitude taken from Ref. [25]. The error bars correspond to statistical uncertainties and boxes to systematic ones.

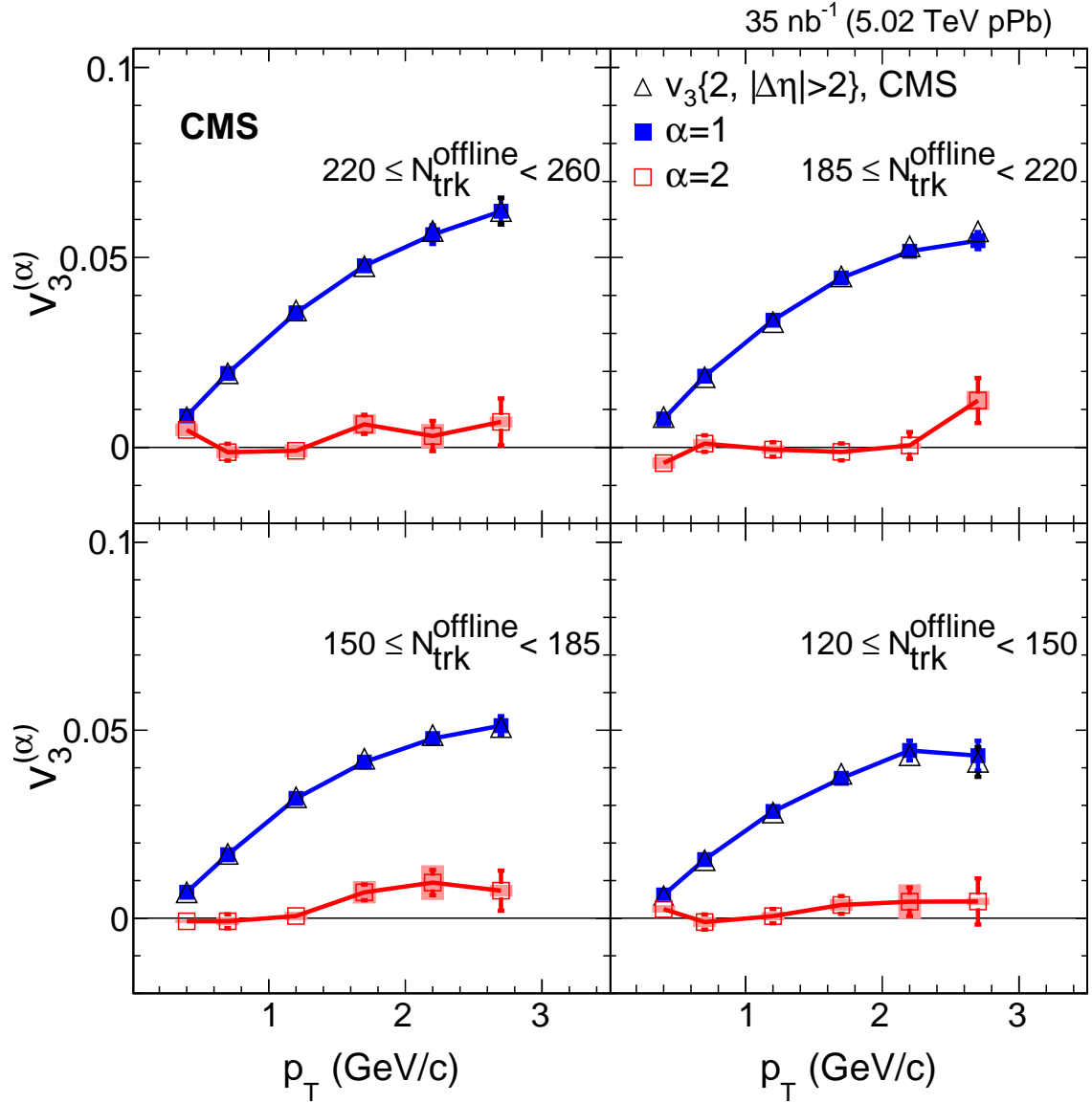


Figure 4: Leading ($\alpha = 1$) and subleading ($\alpha = 2$) modes for $n = 3$ as a function of p_T , measured in high-multiplicity pPb collisions at $\sqrt{s_{\text{NN}}} = 5.02$ TeV, for four classes of reconstructed track multiplicity $N_{\text{trk}}^{\text{offline}}$. The results for the leading mode ($\alpha = 1$) are compared to the standard triangular flow magnitude taken from Ref. [25]. The error bars correspond to statistical uncertainties and boxes to systematic ones.

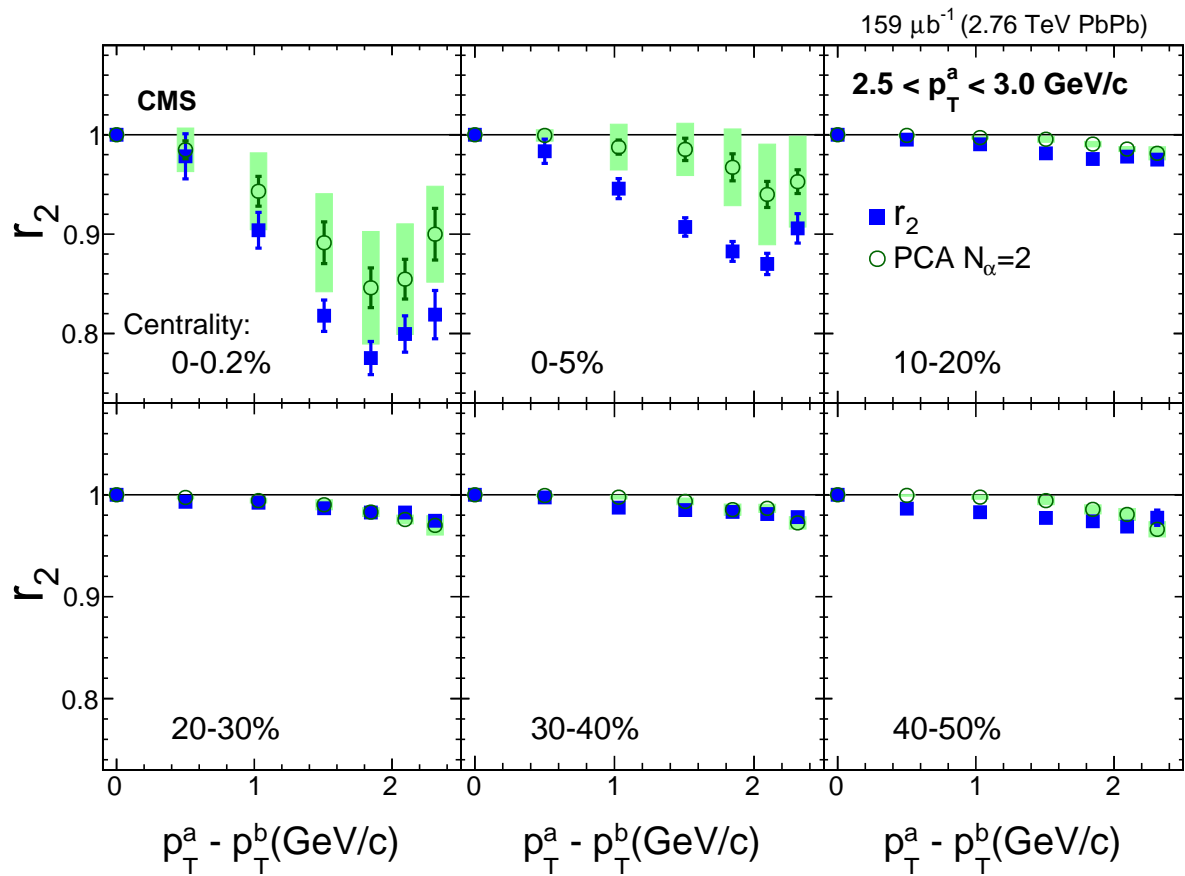


Figure 5: Comparison of the Pearson correlation coefficient r_2 reconstructed with harmonic decomposition using the leading and subleading modes and r_2 values from Ref. [19], as a function of $p_T^a - p_T^b$ in bin of p_T^a for six centrality classes in PbPb collisions at $\sqrt{s_{\text{NN}}} = 2.76$ TeV. The error bars correspond to statistical uncertainties and boxes to systematic ones.

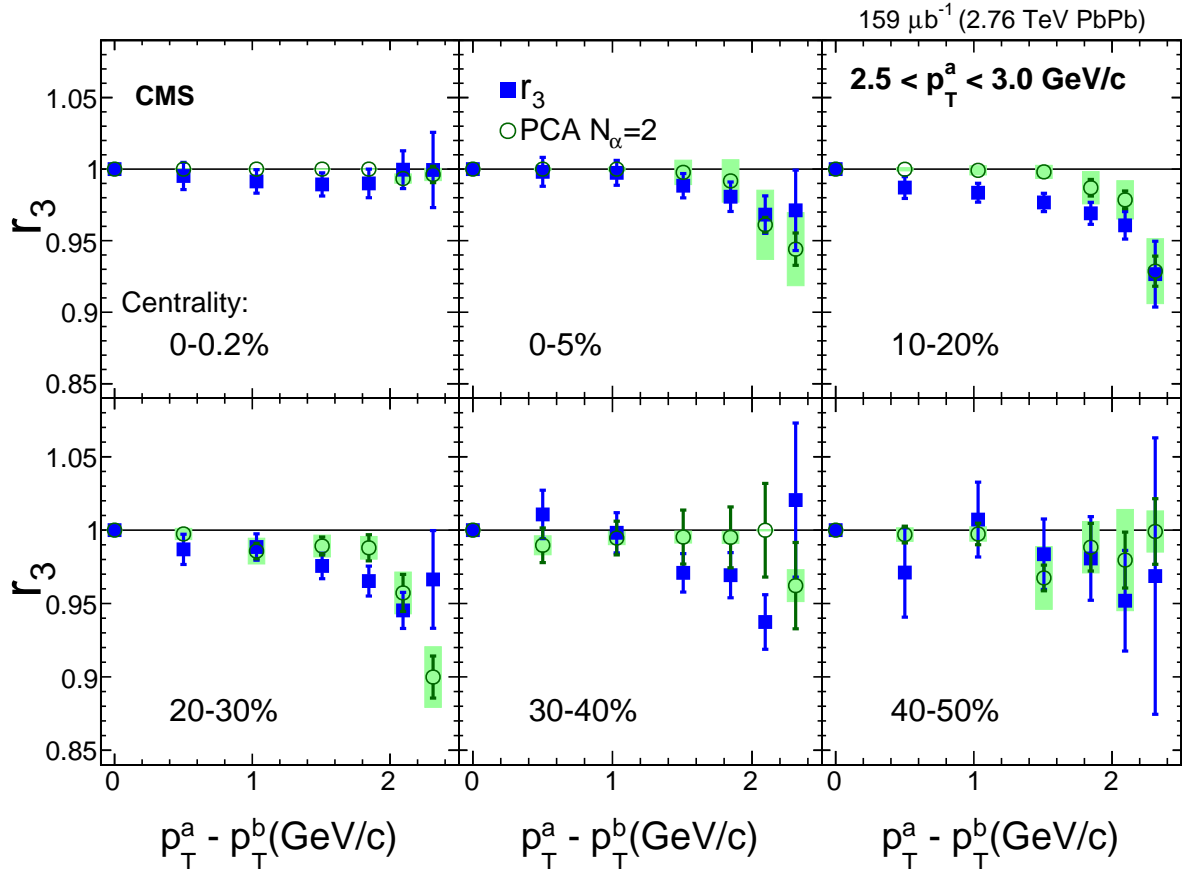


Figure 6: Comparison of the Pearson correlation coefficient r_3 reconstructed with harmonic decomposition using the leading and subleading modes and r_3 values from Ref. [19], as a function of $p_T^a - p_T^b$ in bin of p_T^a for six centrality classes in PbPb collisions at $\sqrt{s_{\text{NN}}} = 2.76$ TeV. The error bars correspond to statistical uncertainties and boxes to systematic ones.

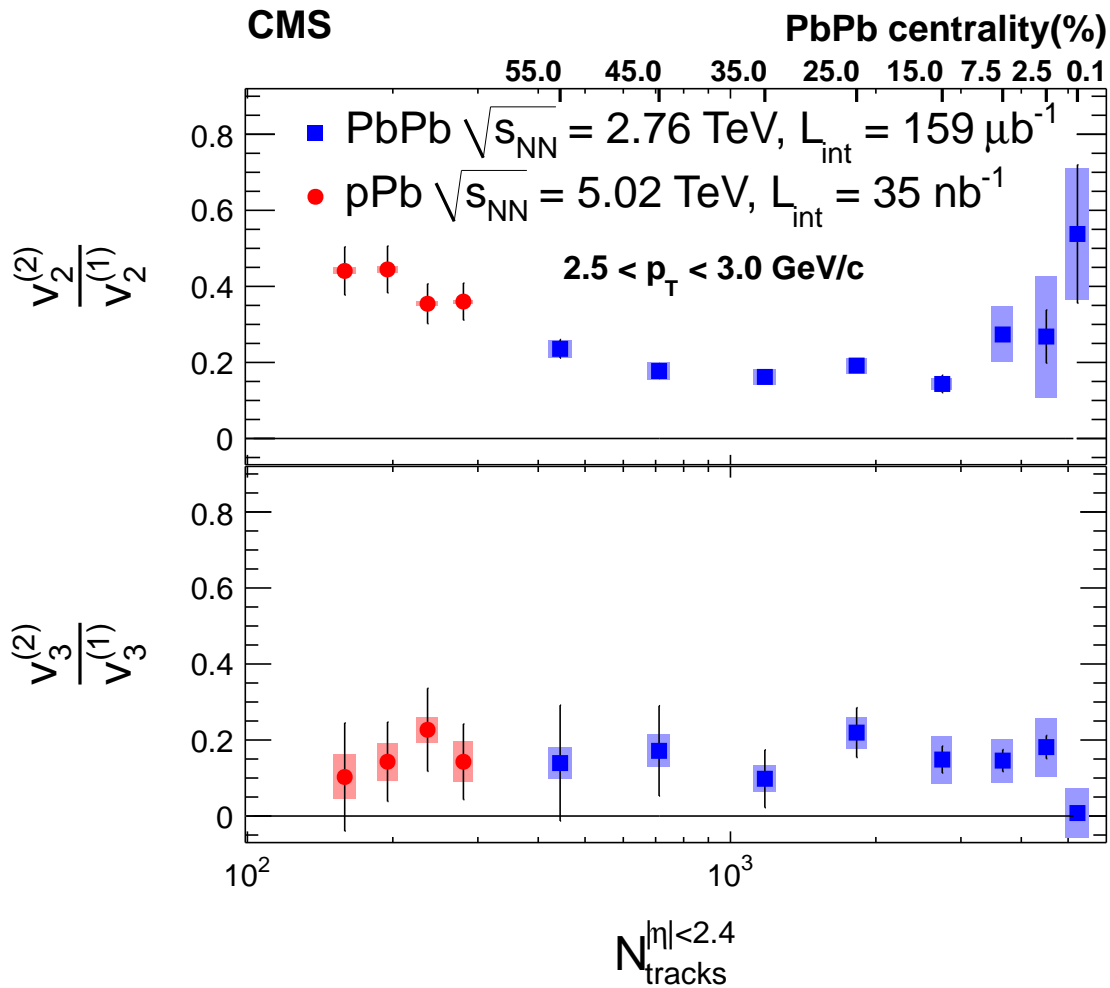


Figure 7: The ratio between values of the subleading and leading modes, taken for the highest p_T bin, as a function of centrality and of charged-particle multiplicity at midrapidity (double axis). The PCA flow results for PbPb collisions at $\sqrt{s_{NN}} = 2.76 \text{ TeV}$ (filled blue squares) and for pPb collisions at $\sqrt{s_{NN}} = 5.02 \text{ TeV}$ (filled red circles). The error bars correspond to statistical uncertainties and boxes to systematic ones.

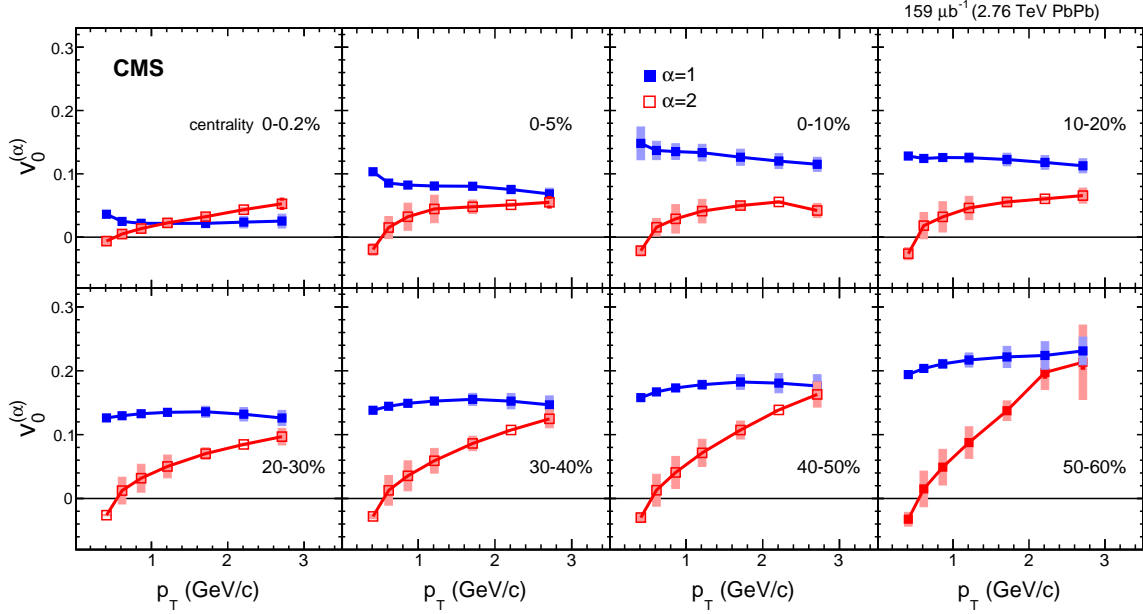


Figure 8: Leading and subleading modes for $n = 0$, i.e. fluctuations in the total multiplicity, spanning eight centralities in PbPb collisions at $\sqrt{s_{\text{NN}}} = 2.76$ TeV. The error bars correspond to statistical uncertainties and boxes to systematic ones. The systematic uncertainties are strongly correlated bin-to-bin.

value within a given bin. For comparison, $v_2^{(1)}$ is plotted together with $v_2\{2\}$ from CMS for ultracentral collisions [15] and from ALICE for midcentral collisions [7]. The leading mode, $v_2^{(1)}$, is dominant and is essentially equal to the single-particle anisotropy $v_2\{2\}$ extracted from two-particle correlations. The subleading mode, $v_2^{(2)}$, is nonzero for all centrality classes and it tends to rise with p_T . It has a small magnitude of about 0.02 for the highest p_T bin and more central collisions and then gradually increases up to 0.05 towards peripheral collisions.

Figure 2 shows leading and subleading modes for the triangular case ($n = 3$), using the same eight centrality classes in PbPb collisions at $\sqrt{s_{\text{NN}}} = 2.76$ TeV. Similar to the $n = 2$ case, $v_3^{(1)}$ is plotted together with $v_3\{2\}$ from CMS for ultracentral collisions [15] and from ALICE for midcentral collisions [7]. A very good agreement is found between $v_3^{(1)}$ and the standard $v_3\{2\}$. The subleading mode, $v_3^{(2)}$, is practically zero for ultracentral collisions but shows positive values for a range of centralities at high p_T . From a hydrodynamical point of view the existence of the subleading mode for $n = 3$ is the response to the first radial excitation of triangularity [32].

Figure 3 shows leading and subleading modes in the case of the elliptic harmonic ($n = 2$) in pPb collisions at $\sqrt{s_{\text{NN}}} = 5.02$ TeV as a function of p_T for four different classes of multiplicity. The data are binned into six p_T bins covering the region $0.3 < p_T < 3.0$ GeV/c. The number of differential p_T bins for constructing the covariance matrix is $N_\alpha = 6$. As seen in PbPb collisions, the leading mode is equal to standard $v_2\{2\}$ CMS results from Ref. [25]. Looking at the subleading mode ($\alpha = 2$) values close to zero are observed at low p_T with a moderate increase in magnitude towards high p_T . For p_T values close to 3.0 GeV/c the subleading mode $v_2^{(2)}$ has a significant nonzero magnitude. This is the same p_T region where the biggest factoriza-

tion breaking has been seen in high-multiplicity pPb collisions [19]. For both the leading and subleading elliptic modes, the data shows little multiplicity dependence for pPb collisions.

Figure 4 shows leading and subleading modes for the triangular case ($n = 3$) for the same multiplicity intervals from high-multiplicity pPb collisions. As for the PbPb case, the differential values of the standard single-particle anisotropy $v_3\{2\}$ from Ref. [25] and $v_3^{(1)}$ are equal. The bottom panel of Fig. 4 shows that $v_3^{(2)}$ is close to zero for all values of p_T . Quantitatively similar behavior was seen for flow factorization breaking in Ref. [19]. Similarly to the elliptic case, the leading and subleading triangular modes are rather independent of multiplicity for pPb collisions.

The Pearson correlation coefficient defined in Eq. (12) measures the magnitude of factorization breaking. This coefficient depends upon the two-particle harmonics $V_{n\Delta}$ that in turn are built up from the complete set of modes as shown in Eq. (14). These harmonics are approximated by the sum of just the leading and subleading modes. The comparison between the values of the PCA r_2 and of the r_2 from Ref. [19] is shown in Fig. 5. Using only the leading and subleading modes it is possible to reconstruct the shape of the r_2 . However r_2 is closer to unity for the PCA results than for the previous measurements. This is expected because the $V_{n\Delta}$ values are constructed from only two of the modes. Figure 6 shows the $n = 3$ case, again using the comparison with r_3 from the previous two-particle correlation analysis [19]. Although the errors are large it is clear that the principle-component analysis tracks the previously measured divergence of r_3 from unity at high p_T .

The Pearson coefficient calculated from Eq. (12) can be expanded as a power series of ratios of modes. Figure 7 shows the ratio of the leading and subleading modes for both pPb and PbPb collisions as a function of centrality (track multiplicity). The ratios are calculated for the highest p_T bin used in the analysis. The top panel shows the elliptic case while the bottom panel shows the triangular case. For the elliptic case the ratio is clearly above zero, with pPb high-multiplicity values being above the peripheral PbPb ones. For the triangular case half of the individual points are consistent with zero within the uncertainties. However, the ensemble of all the points suggest that the ratio is above zero.

Finally, Fig. 8 shows leading and subleading modes for the multiplicity case ($n = 0$) for PbPb collisions as a function of p_T for eight regions of centrality. For all centralities the leading mode depends only weakly on p_T , while the subleading mode increases rapidly with p_T except for very central collisions. The observed increase of the subleading mode with p_T for all centralities is a response to radial-flow fluctuations [22, 33]. From a hydrodynamical point of view, the number of particles at high- p_T decreases exponentially as $\exp[p_T(u - u_0)/T]$. Here, T is the temperature, u is the maximum fluid velocity, and $u_0 = \sqrt{1 + u^2}$. A small variation in u produces a relative yield that increases linearly with p_T . Such behaviour is observed in the data for more peripheral collisions. At a given p_T the subleading mode increases strongly from central to peripheral collisions. Since peripheral collisions correspond to smaller interaction volumes, it is expected that p_T fluctuations are more important for peripheral than for central events.

7 Summary

For the first time the leading and subleading modes of elliptic and triangular flow have been measured for 5.02 TeV pPb and 2.76 TeV PbPb collisions. For PbPb collisions the leading and subleading modes of multiplicity fluctuations have also been measured. Since the principal component analysis uses all the information encoded in the covariance matrix, it provides in-

creased sensitivity to fluctuations. For a very wide range of p_T and centrality, the leading modes of the elliptic and triangular flow are found to be essentially equal to the anisotropy coefficients measured using the standard two-particle correlation method. For both the elliptic and triangular cases the subleading modes are non-zero and increase with p_T . This behavior reflects a breakdown of flow factorization at high p_T in both the pPb and PbPb systems. For charged-particle multiplicity both the leading and subleading modes increase steadily from central to peripheral PbPb events. The leading mode depends only weakly upon p_T while the subleading mode increases strongly with p_T . This centrality and p_T dependence is suggestive of the presence of fluctuations in the radial flow.

In summary the subleading modes of the principal-component analysis capture new information from the spectra of flow and multiplicity fluctuations and provide an efficient method to quantify the breakdown of factorization in two-particle correlations.

Acknowledgments

We congratulate our colleagues in the CERN accelerator departments for the excellent performance of the LHC and thank the technical and administrative staffs at CERN and at other CMS institutes for their contributions to the success of the CMS effort. In addition, we gratefully acknowledge the computing centers and personnel of the Worldwide LHC Computing Grid for delivering so effectively the computing infrastructure essential to our analyses. Finally, we acknowledge the enduring support for the construction and operation of the LHC and the CMS detector provided by the following funding agencies: BMWFW and FWF (Austria); FNRS and FWO (Belgium); CNPq, CAPES, FAPERJ, and FAPESP (Brazil); MES (Bulgaria); CERN; CAS, MoST, and NSFC (China); COLCIENCIAS (Colombia); MSES and CSF (Croatia); RPF (Cyprus); SENESCYT (Ecuador); MoER, ERC IUT, and ERDF (Estonia); Academy of Finland, MEC, and HIP (Finland); CEA and CNRS/IN2P3 (France); BMBF, DFG, and HGF (Germany); GSRT (Greece); OTKA and NIH (Hungary); DAE and DST (India); IPM (Iran); SFI (Ireland); INFN (Italy); MSIP and NRF (Republic of Korea); LAS (Lithuania); MOE and UM (Malaysia); BUAP, CINVESTAV, CONACYT, LNS, SEP, and UASLP-FAI (Mexico); MBIE (New Zealand); PAEC (Pakistan); MSHE and NSC (Poland); FCT (Portugal); JINR (Dubna); MON, RosAtom, RAS, RFBR and RAEP (Russia); MESTD (Serbia); SEIDI, CPAN, PCTI and FEDER (Spain); Swiss Funding Agencies (Switzerland); MST (Taipei); ThEPCenter, IPST, STAR, and NSTDA (Thailand); TUBITAK and TAEK (Turkey); NASU and SFFR (Ukraine); STFC (United Kingdom); DOE and NSF (USA).

Individuals have received support from the Marie-Curie program and the European Research Council and Horizon 2020 Grant, contract No. 675440 (European Union); the Leventis Foundation; the A. P. Sloan Foundation; the Alexander von Humboldt Foundation; the Belgian Federal Science Policy Office; the Fonds pour la Formation à la Recherche dans l'Industrie et dans l'Agriculture (FRIA-Belgium); the Agentschap voor Innovatie door Wetenschap en Technologie (IWT-Belgium); the Ministry of Education, Youth and Sports (MEYS) of the Czech Republic; the Council of Science and Industrial Research, India; the HOMING PLUS program of the Foundation for Polish Science, cofinanced from European Union, Regional Development Fund, the Mobility Plus program of the Ministry of Science and Higher Education, the National Science Center (Poland), contracts Harmonia 2014/14/M/ST2/00428, Opus 2014/13/B/ST2/02543, 2014/15/B/ST2/03998, and 2015/19/B/ST2/02861, Sonata-bis 2012/07/E/ST2/01406; the National Priorities Research Program by Qatar National Research Fund; the Programa Clarín-COFUND del Principado de Asturias; the Thalís and Aristeia programs cofinanced by EU-ESF and the Greek NSRF; the Rachadapisek Sompot Fund for Postdoctoral Fellowship, Chula-

longkorn University and the Chulalongkorn Academic into Its 2nd Century Project Advancement Project (Thailand); and the Welch Foundation, contract C-1845.

References

- [1] BRAHMS Collaboration, “Quark gluon plasma and color glass condensate at RHIC? The perspective from the BRAHMS experiment”, *Nucl. Phys. A* **757** (2005) 1, doi:10.1016/j.nuclphysa.2005.02.130, arXiv:nucl-ex/0410020.
- [2] PHOBOS Collaboration, “The PHOBOS perspective on discoveries at RHIC”, *Nucl. Phys. A* **757** (2005) 28, doi:10.1016/j.nuclphysa.2005.03.084, arXiv:nucl-ex/0410022.
- [3] STAR Collaboration, “Experimental and theoretical challenges in the search for the Quark Gluon Plasma: The STAR Collaboration’s critical assessment of the evidence from RHIC collisions”, *Nucl. Phys. A* **757** (2005) 102, doi:10.1016/j.nuclphysa.2005.03.085, arXiv:nucl-ex/0501009.
- [4] PHENIX Collaboration, “Formation of dense partonic matter in relativistic nucleus-nucleus collisions at RHIC: Experimental evaluation by the PHENIX collaboration”, *Nucl. Phys. A* **757** (2005) 184, doi:10.1016/j.nuclphysa.2005.03.086, arXiv:nucl-ex/0410003.
- [5] J.-Y. Ollitrault, “Anisotropy as a signature of transverse collective flow”, *Phys. Rev. D* **46** (1992) 2290, doi:10.1103/PhysRevD.46.2290.
- [6] P. F. Kolb, J. Sollfrank, and U. Heinz, “Anisotropic transverse flow and the quark hadron phase transition”, *Phys. Rev. C* **62** (2000) 054909, doi:10.1103/PhysRevC.62.054909, arXiv:hep-ph/0006129.
- [7] ALICE Collaboration, “Harmonic decomposition of two-particle angular correlations in Pb-Pb collisions at $\sqrt{s_{NN}} = 2.76$ TeV”, *Phys. Lett. B* **708** (2012) 249, doi:10.1016/j.physletb.2012.01.060, arXiv:1109.2501.
- [8] ALICE Collaboration, “Elliptic flow of identified hadrons in Pb-Pb collisions at $\sqrt{s_{NN}} = 2.76$ TeV”, *JHEP* **06** (2015) 190, doi:10.1007/JHEP06(2015)190, arXiv:1405.4632.
- [9] ATLAS Collaboration, “Measurement of the azimuthal anisotropy for charged particle production in $\sqrt{s_{NN}} = 2.76$ TeV lead-lead collisions with the ATLAS detector”, *Phys. Rev. C* **86** (2012) 014907, doi:10.1103/PhysRevC.86.014907, arXiv:1203.3087.
- [10] ATLAS Collaboration, “Measurement of the distributions of event-by-event flow harmonics in lead-lead collisions at $\sqrt{s_{NN}} = 2.76$ TeV with the ATLAS detector at the LHC”, *JHEP* **11** (2013) 183, doi:10.1007/JHEP11(2013)183, arXiv:1305.2942.
- [11] ATLAS Collaboration, “Measurement of event-plane correlations in $\sqrt{s_{NN}} = 2.76$ TeV lead-lead collisions with the ATLAS detector”, *Phys. Rev. C* **90** (2014) 024905, doi:10.1103/PhysRevC.90.024905, arXiv:1403.0489.
- [12] CMS Collaboration, “Centrality dependence of dihadron correlations and azimuthal anisotropy harmonics in PbPb collisions at $\sqrt{s_{NN}} = 2.76$ TeV”, *Eur. Phys. J. C* **72** (2012) 2012, doi:10.1140/epjc/s10052-012-2012-3, arXiv:1201.3158.
- [13] CMS Collaboration, “Measurement of the elliptic anisotropy of charged particles produced in PbPb collisions at $\sqrt{s_{NN}} = 2.76$ TeV”, *Phys. Rev. C* **87** (2013) 014902, doi:10.1103/PhysRevC.87.014902, arXiv:1204.1409.

- [14] CMS Collaboration, "Measurement of higher-order harmonic azimuthal anisotropy in PbPb collisions at $\sqrt{s_{\text{NN}}} = 2.76$ TeV", *Phys. Rev. C* **89** (2014) 044906, doi:10.1103/PhysRevC.89.044906, arXiv:1310.8651.
- [15] CMS Collaboration, "Studies of azimuthal dihadron correlations in ultra-central PbPb collisions at $\sqrt{s_{\text{NN}}} = 2.76$ TeV", *JHEP* **02** (2014) 088, doi:10.1007/JHEP02(2014)088, arXiv:1312.1845.
- [16] B. Schenke, S. Jeon, and C. Gale, "(3+1)D hydrodynamic simulation of relativistic heavy-ion collisions", *Phys. Rev. C* **82** (2010) 014903, doi:10.1103/PhysRevC.82.014903, arXiv:1004.1408.
- [17] C. Shen et al., "The iEBE-VISHNU code package for relativistic heavy-ion collisions", *Comput. Phys. Commun.* **199** (2016) 61, doi:10.1016/j.cpc.2015.08.039, arXiv:1409.8164.
- [18] K. Dusling and D. Teaney, "Simulating elliptic flow with viscous hydrodynamics", *Phys. Rev. C* **77** (2008) 034905, doi:10.1103/PhysRevC.77.034905, arXiv:0710.5932.
- [19] CMS Collaboration, "Evidence for transverse momentum and pseudorapidity dependent event plane fluctuations in PbPb and pPb collisions", *Phys. Rev. C* **92** (2015) 034911, doi:10.1103/PhysRevC.92.034911, arXiv:1503.01692.
- [20] F. G. Gardim, F. Grassi, M. Luzum, and J.-Y. Ollitrault, "Breaking of factorization of two-particle correlations in hydrodynamics", *Phys. Rev. C* **87** (2013) 031901, doi:10.1103/PhysRevC.87.031901, arXiv:1211.0989.
- [21] U. Heinz, Z. Qiu, and C. Shen, "Fluctuating flow angles and anisotropic flow measurements", *Phys. Rev. C* **87** (2013) 034913, doi:10.1103/PhysRevC.87.034913, arXiv:1302.3535.
- [22] R. S. Bhalerao, J.-Y. Ollitrault, S. Pal, and D. Teaney, "Principal component analysis of event-by-event fluctuations", *Phys. Rev. Lett.* **114** (2015) 152301, doi:10.1103/PhysRevLett.114.152301, arXiv:1410.7739.
- [23] O. A. Grachov et al., "Performance of the combined zero degree calorimeter for CMS", in *XIII Int. Conf. on Calorimetry in High Energy Physics (CALOR 2008)*, edited by Michele Livan. arXiv:0807.0785. *J. Phys.: Conf. Series*, 160 (2009) 012059. doi:10.1088/1742-6596/160/1/012059.
- [24] CMS Collaboration, "The CMS experiment at the CERN LHC", *JINST* **3** (2008) S08004, doi:10.1088/1748-0221/3/08/S08004.
- [25] CMS Collaboration, "Multiplicity and transverse momentum dependence of two- and four-particle correlations in pPb and PbPb collisions", *Phys. Lett. B* **724** (2013) 213, doi:10.1016/j.physletb.2013.06.028, arXiv:1305.0609.
- [26] Ø. Djuvsland and J. Nystrand, "Single and double photonuclear excitations in Pb+Pb collisions at $\sqrt{s_{\text{NN}}} = 2.76$ TeV at the CERN Large Hadron Collider", *Phys. Rev. C* **83** (2011) 041901, doi:10.1103/PhysRevC.83.041901, arXiv:1011.4908.
- [27] I. P. Lokhtin and A. M. Snigirev, "A model of jet quenching in ultrarelativistic heavy ion collisions and high- p_T hadron spectra at RHIC", *Eur. Phys. J. C* **45** (2005) 211, doi:10.1140/epjc/s2005-02426-3, arXiv:nucl-ex/0506189.

- [28] S. Porteboeuf, T. Pierog, and K. Werner, "Producing hard processes regarding the complete event: The EPOS event generator", (2011). [arXiv:1006.2967](#).
- [29] M. Gyulassy and X.-N. Wang, "HIJING 1.0: A Monte Carlo program for parton and particle production in high energy hadronic and nuclear collisions", *Comput. Phys. Commun.* **83** (1994) 307, [doi:10.1016/0010-4655\(94\)90057-4](#), [arXiv:nucl-th/9502021](#).
- [30] CMS Collaboration, "Tracking and vertexing results from first collisions", CMS Physics Analysis Summary CMS-PAS-TRK-10-001, 2010.
- [31] A. Mazeliauskas and D. Teaney, "Fluctuations of harmonic and radial flow in heavy ion collisions with principal components", *Phys. Rev. C* **93** (2016) 024913, [doi:10.1103/PhysRevC.93.024913](#), [arXiv:1509.07492](#).
- [32] A. Mazeliauskas and D. Teaney, "Subleading harmonic flows in hydrodynamic simulations of heavy ion collisions", *Phys. Rev. C* **91** (2015) 044902, [doi:10.1103/PhysRevC.91.044902](#), [arXiv:1501.03138](#).
- [33] N. Borghini and J.-Y. Ollitrault, "Momentum spectra, anisotropic flow, and ideal fluids", *Phys. Lett. B* **642** (2006) 227, [doi:10.1016/j.physletb.2006.09.062](#), [arXiv:nucl-ex/0506045](#).

A The CMS Collaboration

Yerevan Physics Institute, Yerevan, Armenia

A.M. Sirunyan, A. Tumasyan

Institut für Hochenergiephysik, Wien, Austria

W. Adam, F. Ambrogio, E. Asilar, T. Bergauer, J. Brandstetter, E. Brondolin, M. Dragicevic, J. Erö, M. Flechl, M. Friedl, R. Frühwirth¹, V.M. Ghete, J. Grossmann, J. Hrubec, M. Jeitler¹, A. König, N. Krammer, I. Krätschmer, D. Liko, T. Madlener, I. Mikulec, E. Pree, D. Rabady, N. Rad, H. Rohringer, J. Schieck¹, R. Schöfbeck, M. Spanring, D. Spitzbart, J. Strauss, W. Waltenberger, J. Wittmann, C.-E. Wulz¹, M. Zarucki

Institute for Nuclear Problems, Minsk, Belarus

V. Chekhovsky, V. Mossolov, J. Suarez Gonzalez

Universiteit Antwerpen, Antwerpen, Belgium

E.A. De Wolf, X. Janssen, J. Lauwers, M. Van De Klundert, H. Van Haevermaet, P. Van Mechelen, N. Van Remortel, A. Van Spilbeeck

Vrije Universiteit Brussel, Brussel, Belgium

S. Abu Zeid, F. Blekman, J. D'Hondt, I. De Bruyn, J. De Clercq, K. Deroover, G. Flouris, S. Lowette, S. Moortgat, L. Moreels, A. Olbrechts, Q. Python, K. Skovpen, S. Tavernier, W. Van Doninck, P. Van Mulders, I. Van Parijs

Université Libre de Bruxelles, Bruxelles, Belgium

H. Brun, B. Clerbaux, G. De Lentdecker, H. Delannoy, G. Fasanella, L. Favart, R. Goldouzian, A. Grebenyuk, G. Karapostoli, T. Lenzi, J. Luetic, T. Maerschalk, A. Marinov, A. Randle-conde, T. Seva, C. Vander Velde, P. Vanlaer, D. Vannerom, R. Yonamine, F. Zenoni, F. Zhang²

Ghent University, Ghent, Belgium

A. Cimmino, T. Cornelis, D. Dobur, A. Fagot, M. Gul, I. Khvastunov, D. Poyraz, C. Roskas, S. Salva, M. Tytgat, W. Verbeke, N. Zaganidis

Université Catholique de Louvain, Louvain-la-Neuve, Belgium

H. Bakhshiansohi, O. Bondu, S. Brochet, G. Bruno, A. Caudron, S. De Visscher, C. Delaere, M. Delcourt, B. Francois, A. Giammanco, A. Jafari, M. Komm, G. Krintiras, V. Lemaitre, A. Magitteri, A. Mertens, M. Musich, K. Piotrkowski, L. Quertenmont, M. Vidal Marono, S. Wertz

Université de Mons, Mons, Belgium

N. Bely

Centro Brasileiro de Pesquisas Fisicas, Rio de Janeiro, Brazil

W.L. Aldá Júnior, F.L. Alves, G.A. Alves, L. Brito, M. Correa Martins Junior, C. Hensel, A. Moraes, M.E. Pol, P. Rebello Teles

Universidade do Estado do Rio de Janeiro, Rio de Janeiro, Brazil

E. Belchior Batista Das Chagas, W. Carvalho, J. Chinellato³, A. Custódio, E.M. Da Costa, G.G. Da Silveira⁴, D. De Jesus Damiao, S. Fonseca De Souza, L.M. Huertas Guativa, H. Malbouisson, M. Melo De Almeida, C. Mora Herrera, L. Mundim, H. Nogima, A. Santoro, A. Sznajder, E.J. Tonelli Manganote³, F. Torres Da Silva De Araujo, A. Vilela Pereira

Universidade Estadual Paulista ^a, Universidade Federal do ABC ^b, São Paulo, Brazil

S. Ahuja^a, C.A. Bernardes^a, T.R. Fernandez Perez Tomei^a, E.M. Gregores^b, P.G. Mercadante^b, C.S. Moon^a, S.F. Novaes^a, Sandra S. Padula^a, D. Romero Abad^b, J.C. Ruiz Vargas^a

Institute for Nuclear Research and Nuclear Energy of Bulgaria Academy of Sciences

A. Aleksandrov, R. Hadjiiska, P. Iaydjiev, M. Misheva, M. Rodozov, S. Stoykova, G. Sultanov, M. Vutova

University of Sofia, Sofia, Bulgaria

A. Dimitrov, I. Glushkov, L. Litov, B. Pavlov, P. Petkov

Beihang University, Beijing, China

W. Fang⁵, X. Gao⁵

Institute of High Energy Physics, Beijing, China

M. Ahmad, J.G. Bian, G.M. Chen, H.S. Chen, M. Chen, Y. Chen, C.H. Jiang, D. Leggat, Z. Liu, F. Romeo, S.M. Shaheen, A. Spiezia, J. Tao, C. Wang, Z. Wang, E. Yazgan, H. Zhang, J. Zhao

State Key Laboratory of Nuclear Physics and Technology, Peking University, Beijing, China

Y. Ban, G. Chen, Q. Li, S. Liu, Y. Mao, S.J. Qian, D. Wang, Z. Xu

Universidad de Los Andes, Bogota, Colombia

C. Avila, A. Cabrera, L.F. Chaparro Sierra, C. Florez, C.F. González Hernández, J.D. Ruiz Alvarez

University of Split, Faculty of Electrical Engineering, Mechanical Engineering and Naval Architecture, Split, Croatia

B. Courbon, N. Godinovic, D. Lelas, I. Puljak, P.M. Ribeiro Cipriano, T. Sculac

University of Split, Faculty of Science, Split, Croatia

Z. Antunovic, M. Kovac

Institute Rudjer Boskovic, Zagreb, Croatia

V. Brigljevic, D. Ferencek, K. Kadija, B. Mesic, T. Susa

University of Cyprus, Nicosia, Cyprus

M.W. Ather, A. Attikis, G. Mavromanolakis, J. Mousa, C. Nicolaou, F. Ptochos, P.A. Razis, H. Rykaczewski

Charles University, Prague, Czech Republic

M. Finger⁶, M. Finger Jr.⁶

Universidad San Francisco de Quito, Quito, Ecuador

E. Carrera Jarrin

Academy of Scientific Research and Technology of the Arab Republic of Egypt, Egyptian Network of High Energy Physics, Cairo, Egypt

A.A. Abdelalim^{7,8}, Y. Mohammed⁹, E. Salama^{10,11}

National Institute of Chemical Physics and Biophysics, Tallinn, Estonia

R.K. Dewanjee, M. Kadastik, L. Perrini, M. Raidal, A. Tiko, C. Veelken

Department of Physics, University of Helsinki, Helsinki, Finland

P. Eerola, J. Pekkanen, M. Voutilainen

Helsinki Institute of Physics, Helsinki, Finland

J. Härkönen, T. Järvinen, V. Karimäki, R. Kinnunen, T. Lampén, K. Lassila-Perini, S. Lehti, T. Lindén, P. Luukka, E. Tuominen, J. Tuominiemi, E. Tuovinen

Lappeenranta University of Technology, Lappeenranta, Finland

J. Talvitie, T. Tuuva

IRFU, CEA, Université Paris-Saclay, Gif-sur-Yvette, France

M. Besancon, F. Couderc, M. Dejardin, D. Denegri, J.L. Faure, F. Ferri, S. Ganjour, S. Ghosh, A. Givernaud, P. Gras, G. Hamel de Monchenault, P. Jarry, I. Kucher, E. Locci, M. Machet, J. Malcles, G. Negro, J. Rander, A. Rosowsky, M.Ö. Sahin, M. Titov

Laboratoire Leprince-Ringuet, Ecole polytechnique, CNRS/IN2P3, Université Paris-Saclay, Palaiseau, France

A. Abdulsalam, I. Antropov, S. Baffioni, F. Beaudette, P. Busson, L. Cadamuro, C. Charlot, O. Davignon, R. Granier de Cassagnac, M. Jo, S. Lisniak, A. Lobanov, J. Martin Blanco, M. Nguyen, C. Ochando, G. Ortona, P. Paganini, P. Pigard, S. Regnard, R. Salerno, J.B. Sauvan, Y. Sirois, A.G. Stahl Leiton, T. Strebler, Y. Yilmaz, A. Zabi, A. Zghiche

Université de Strasbourg, CNRS, IPHC UMR 7178, F-67000 Strasbourg, France

J.-L. Agram¹², J. Andrea, D. Bloch, J.-M. Brom, M. Buttignol, E.C. Chabert, N. Chanon, C. Collard, E. Conte¹², X. Coubez, J.-C. Fontaine¹², D. Gelé, U. Goerlach, M. Jansová, A.-C. Le Bihan, P. Van Hove

Centre de Calcul de l'Institut National de Physique Nucleaire et de Physique des Particules, CNRS/IN2P3, Villeurbanne, France

S. Gadrat

Université de Lyon, Université Claude Bernard Lyon 1, CNRS-IN2P3, Institut de Physique Nucléaire de Lyon, Villeurbanne, France

S. Beauceron, C. Bernet, G. Boudoul, R. Chierici, D. Contardo, P. Depasse, H. El Mamouni, J. Fay, L. Finco, S. Gascon, M. Gouzevitch, G. Grenier, B. Ille, F. Lagarde, I.B. Laktineh, M. Lethuillier, L. Mirabito, A.L. Pequegnot, S. Perries, A. Popov¹³, V. Sordini, M. Vander Donckt, S. Viret

Georgian Technical University, Tbilisi, Georgia

T. Toriashvili¹⁴

Tbilisi State University, Tbilisi, Georgia

Z. Tsamalaidze⁶

RWTH Aachen University, I. Physikalisches Institut, Aachen, Germany

C. Autermann, S. Beranek, L. Feld, M.K. Kiesel, K. Klein, M. Lipinski, M. Preuten, C. Schomakers, J. Schulz, T. Verlage

RWTH Aachen University, III. Physikalisches Institut A, Aachen, Germany

A. Albert, M. Brodski, E. Dietz-Laursonn, D. Duchardt, M. Endres, M. Erdmann, S. Erdweg, T. Esch, R. Fischer, A. Güth, M. Hamer, T. Hebbeker, C. Heidemann, K. Hoepfner, S. Knutzen, M. Merschmeyer, A. Meyer, P. Millet, S. Mukherjee, M. Olschewski, K. Padeken, T. Pook, M. Radziej, H. Reithler, M. Rieger, F. Scheuch, D. Teyssier, S. Thüer

RWTH Aachen University, III. Physikalisches Institut B, Aachen, Germany

G. Flügge, B. Kargoll, T. Kress, A. Künsken, J. Lingemann, T. Müller, A. Nehr Korn, A. Nowack, C. Pistone, O. Pooth, A. Stahl¹⁵

Deutsches Elektronen-Synchrotron, Hamburg, Germany

M. Aldaya Martin, T. Arndt, C. Asawatangkuldee, K. Beernaert, O. Behnke, U. Behrens, A.A. Bin Anuar, K. Borras¹⁶, V. Botta, A. Campbell, P. Connor, C. Contreras-Campana, F. Costanza, C. Diez Pardos, G. Eckerlin, D. Eckstein, T. Eichhorn, E. Eren, E. Gallo¹⁷, J. Garay Garcia, A. Geiser, A. Gizhko, J.M. Grados Luyando, A. Grohsjean, P. Gunnellini, A. Harb, J. Hauk, M. Hempel¹⁸, H. Jung, A. Kalogeropoulos, M. Kasemann, J. Keaveney, C. Kleinwort,

I. Korol, D. Krücker, W. Lange, A. Lelek, T. Lenz, J. Leonard, K. Lipka, W. Lohmann¹⁸, R. Mankel, I.-A. Melzer-Pellmann, A.B. Meyer, G. Mittag, J. Mnich, A. Mussgiller, E. Ntomari, D. Pitzl, R. Placakyte, A. Raspereza, B. Roland, M. Savitskyi, P. Saxena, R. Shevchenko, S. Spannagel, N. Stefaniuk, G.P. Van Onsem, R. Walsh, Y. Wen, K. Wichmann, C. Wissing, O. Zenaiev

University of Hamburg, Hamburg, Germany

S. Bein, V. Blobel, M. Centis Vignali, A.R. Draeger, T. Dreyer, E. Garutti, D. Gonzalez, J. Haller, M. Hoffmann, A. Junkes, R. Klanner, R. Kogler, N. Kovalchuk, S. Kurz, T. Lapsien, I. Marchesini, D. Marconi, M. Meyer, M. Niedziela, D. Nowatschin, F. Pantaleo¹⁵, T. Peiffer, A. Perieanu, C. Scharf, P. Schleper, A. Schmidt, S. Schumann, J. Schwandt, J. Sonneveld, H. Stadie, G. Steinbrück, F.M. Stober, M. Stöver, H. Tholen, D. Troendle, E. Usai, L. Vanelderen, A. Vanhoefer, B. Vormwald

Institut für Experimentelle Kernphysik, Karlsruhe, Germany

M. Akbiyik, C. Barth, S. Baur, E. Butz, R. Caspart, T. Chwalek, F. Colombo, W. De Boer, A. Dierlamm, B. Freund, R. Friese, M. Giffels, A. Gilbert, D. Haitz, F. Hartmann¹⁵, S.M. Heindl, U. Husemann, F. Kassel¹⁵, S. Kudella, H. Mildner, M.U. Mozer, Th. Müller, M. Plagge, G. Quast, K. Rabbertz, M. Schröder, I. Shvetsov, G. Sieber, H.J. Simonis, R. Ulrich, S. Wayand, M. Weber, T. Weiler, S. Williamson, C. Wöhrmann, R. Wolf

Institute of Nuclear and Particle Physics (INPP), NCSR Demokritos, Aghia Paraskevi, Greece

G. Anagnostou, G. Daskalakis, T. Gerasis, V.A. Giakoumopoulou, A. Kyriakis, D. Loukas, I. Topsis-Giotis

National and Kapodistrian University of Athens, Athens, Greece

S. Kesisoglou, A. Panagiotou, N. Saoulidou

University of Ioánnina, Ioánnina, Greece

I. Evangelou, C. Foudas, P. Kokkas, N. Manthos, I. Papadopoulos, E. Paradas, J. Strologas, F.A. Triantis

MTA-ELTE Lendület CMS Particle and Nuclear Physics Group, Eötvös Loránd University, Budapest, Hungary

M. Csanad, N. Filipovic, G. Pasztor

Wigner Research Centre for Physics, Budapest, Hungary

G. Bencze, C. Hajdu, D. Horvath¹⁹, F. Sikler, V. Veszpremi, G. Vesztergombi²⁰, A.J. Zsigmond

Institute of Nuclear Research ATOMKI, Debrecen, Hungary

N. Beni, S. Czellar, J. Karancsi²¹, A. Makovec, J. Molnar, Z. Szillasi

Institute of Physics, University of Debrecen, Debrecen, Hungary

M. Bartók²⁰, P. Raics, Z.L. Trocsanyi, B. Ujvari

Indian Institute of Science (IISc), Bangalore, India

S. Choudhury, J.R. Komaragiri

National Institute of Science Education and Research, Bhubaneswar, India

S. Bahinipati²², S. Bhowmik, P. Mal, K. Mandal, A. Nayak²³, D.K. Sahoo²², N. Sahoo, S.K. Swain

Panjab University, Chandigarh, India

S. Bansal, S.B. Beri, V. Bhatnagar, U. Bhawandeep, R. Chawla, N. Dhingra, A.K. Kalsi, A. Kaur, M. Kaur, R. Kumar, P. Kumari, A. Mehta, M. Mittal, J.B. Singh, G. Walia

University of Delhi, Delhi, India

Ashok Kumar, Aashaq Shah, A. Bhardwaj, S. Chauhan, B.C. Choudhary, R.B. Garg, S. Keshri, A. Kumar, S. Malhotra, M. Naimuddin, K. Ranjan, R. Sharma, V. Sharma

Saha Institute of Nuclear Physics, HBNI, Kolkata, India

R. Bhardwaj, R. Bhattacharya, S. Bhattacharya, S. Dey, S. Dutt, S. Dutta, S. Ghosh, N. Majumdar, A. Modak, K. Mondal, S. Mukhopadhyay, S. Nandan, A. Purohit, A. Roy, D. Roy, S. Roy Chowdhury, S. Sarkar, M. Sharan, S. Thakur

Indian Institute of Technology Madras, Madras, India

P.K. Behera

Bhabha Atomic Research Centre, Mumbai, India

R. Chudasama, D. Dutta, V. Jha, V. Kumar, A.K. Mohanty¹⁵, P.K. Netrakanti, L.M. Pant, P. Shukla, A. Topkar

Tata Institute of Fundamental Research-A, Mumbai, India

T. Aziz, S. Dugad, B. Mahakud, S. Mitra, G.B. Mohanty, B. Parida, N. Sur, B. Sutar

Tata Institute of Fundamental Research-B, Mumbai, India

S. Banerjee, S. Bhattacharya, S. Chatterjee, P. Das, M. Guchait, Sa. Jain, S. Kumar, M. Maity²⁴, G. Majumder, K. Mazumdar, T. Sarkar²⁴, N. Wickramage²⁵

Indian Institute of Science Education and Research (IISER), Pune, India

S. Chauhan, S. Dube, V. Hegde, A. Kapoor, K. Kothekar, S. Pandey, A. Rane, S. Sharma

Institute for Research in Fundamental Sciences (IPM), Tehran, Iran

S. Chenarani²⁶, E. Eskandari Tadavani, S.M. Etesami²⁶, M. Khakzad, M. Mohammadi Najafabadi, M. Naseri, S. Paktinat Mehdiabadi²⁷, F. Rezaei Hosseinabadi, B. Safarzadeh²⁸, M. Zeinali

University College Dublin, Dublin, Ireland

M. Felcini, M. Grunewald

INFN Sezione di Bari ^a, Università di Bari ^b, Politecnico di Bari ^c, Bari, Italy

M. Abbrescia^{a,b}, C. Calabria^{a,b}, C. Caputo^{a,b}, A. Colaleo^a, D. Creanza^{a,c}, L. Cristella^{a,b}, N. De Filippis^{a,c}, M. De Palma^{a,b}, F. Errico^{a,b}, L. Fiore^a, G. Iaselli^{a,c}, G. Maggi^{a,c}, M. Maggi^a, G. Miniello^{a,b}, S. My^{a,b}, S. Nuzzo^{a,b}, A. Pompili^{a,b}, G. Pugliese^{a,c}, R. Radogna^{a,b}, A. Ranieri^a, G. Selvaggi^{a,b}, A. Sharma^a, L. Silvestris^{a,15}, R. Venditti^a, P. Verwilligen^a

INFN Sezione di Bologna ^a, Università di Bologna ^b, Bologna, Italy

G. Abbiendi^a, C. Battilana, D. Bonacorsi^{a,b}, S. Braibant-Giacomelli^{a,b}, L. Brigliadori^{a,b}, R. Campanini^{a,b}, P. Capiluppi^{a,b}, A. Castro^{a,b}, F.R. Cavallo^a, S.S. Chhibra^{a,b}, G. Codispoti^{a,b}, M. Cuffiani^{a,b}, G.M. Dallavalle^a, F. Fabbri^a, A. Fanfani^{a,b}, D. Fasanella^{a,b}, P. Giacomelli^a, L. Guiducci^{a,b}, S. Marcellini^a, G. Masetti^a, F.L. Navarria^{a,b}, A. Perrotta^a, A.M. Rossi^{a,b}, T. Rovelli^{a,b}, G.P. Siroli^{a,b}, N. Tosi^{a,b,15}

INFN Sezione di Catania ^a, Università di Catania ^b, Catania, Italy

S. Albergo^{a,b}, S. Costa^{a,b}, A. Di Mattia^a, F. Giordano^{a,b}, R. Potenza^{a,b}, A. Tricomi^{a,b}, C. Tuve^{a,b}

INFN Sezione di Firenze ^a, Università di Firenze ^b, Firenze, Italy

G. Barbagli^a, K. Chatterjee^{a,b}, V. Ciulli^{a,b}, C. Civinini^a, R. D'Alessandro^{a,b}, E. Focardi^{a,b}, P. Lenzi^{a,b}, M. Meschini^a, S. Paoletti^a, L. Russo^{a,29}, G. Sguazzoni^a, D. Strom^a, L. Viliani^{a,b,15}

INFN Laboratori Nazionali di Frascati, Frascati, Italy

L. Benussi, S. Bianco, F. Fabbri, D. Piccolo, F. Primavera¹⁵

INFN Sezione di Genova ^a, Università di Genova ^b, Genova, ItalyV. Calvelli^{a,b}, F. Ferro^a, E. Robutti^a, S. Tosi^{a,b}**INFN Sezione di Milano-Bicocca ^a, Università di Milano-Bicocca ^b, Milano, Italy**L. Brianza^{a,b}, F. Brivio^{a,b}, V. Ciriolo^{a,b}, M.E. Dinardo^{a,b}, S. Fiorendi^{a,b}, S. Gennai^a, A. Ghezzi^{a,b}, P. Govoni^{a,b}, M. Malberti^{a,b}, S. Malvezzi^a, R.A. Manzoni^{a,b}, D. Menasce^a, L. Moroni^a, M. Paganoni^{a,b}, K. Pauwels^{a,b}, D. Pedrini^a, S. Pigazzini^{a,b,30}, S. Ragazzi^{a,b}, T. Tabarelli de Fatis^{a,b}**INFN Sezione di Napoli ^a, Università di Napoli 'Federico II' ^b, Napoli, Italy, Università della Basilicata ^c, Potenza, Italy, Università G. Marconi ^d, Roma, Italy**S. Buontempo^a, N. Cavallo^{a,c}, S. Di Guida^{a,d,15}, F. Fabozzi^{a,c}, F. Fienga^{a,b}, A.O.M. Iorio^{a,b}, W.A. Khan^a, L. Lista^a, S. Meola^{a,d,15}, P. Paolucci^{a,15}, C. Sciacca^{a,b}, F. Thyssen^a**INFN Sezione di Padova ^a, Università di Padova ^b, Padova, Italy, Università di Trento ^c, Trento, Italy**P. Azzi^{a,15}, N. Bacchetta^a, L. Benato^{a,b}, D. Bisello^{a,b}, A. Boletti^{a,b}, P. Checchia^a, M. Dall'Osso^{a,b}, P. De Castro Manzano^a, T. Dorigo^a, U. Dosselli^a, F. Gasparini^{a,b}, A. Gozzelino^a, S. Lacaprara^a, M. Margoni^{a,b}, A.T. Meneguzzo^{a,b}, M. Michelotto^a, F. Montecassiano^a, D. Pantano^a, N. Pozzobon^{a,b}, P. Ronchese^{a,b}, R. Rossin^{a,b}, F. Simonetto^{a,b}, E. Torassa^a, M. Zanetti^{a,b}, P. Zotto^{a,b}, G. Zumerle^{a,b}**INFN Sezione di Pavia ^a, Università di Pavia ^b, Pavia, Italy**A. Braghieri^a, F. Fallavollita^{a,b}, A. Magnani^{a,b}, P. Montagna^{a,b}, S.P. Ratti^{a,b}, V. Re^a, M. Ressegotti, C. Riccardi^{a,b}, P. Salvini^a, I. Vai^{a,b}, P. Vitulo^{a,b}**INFN Sezione di Perugia ^a, Università di Perugia ^b, Perugia, Italy**L. Alunni Solestizi^{a,b}, G.M. Bilei^a, D. Ciangottini^{a,b}, L. Fanò^{a,b}, P. Lariccia^{a,b}, R. Leonardi^{a,b}, G. Mantovani^{a,b}, V. Mariani^{a,b}, M. Menichelli^a, A. Saha^a, A. Santocchia^{a,b}, D. Spiga**INFN Sezione di Pisa ^a, Università di Pisa ^b, Scuola Normale Superiore di Pisa ^c, Pisa, Italy**K. Androsov^a, P. Azzurri^{a,15}, G. Bagliesi^a, J. Bernardini^a, T. Boccali^a, L. Borrello, R. Castaldi^a, M.A. Ciocci^{a,b}, R. Dell'Orso^a, G. Fedi^a, A. Giassi^a, M.T. Grippo^{a,29}, F. Ligabue^{a,c}, T. Lomtadze^a, L. Martini^{a,b}, A. Messineo^{a,b}, F. Palla^a, A. Rizzi^{a,b}, A. Savoy-Navarro^{a,31}, P. Spagnolo^a, R. Tenchini^a, G. Tonelli^{a,b}, A. Venturi^a, P.G. Verdini^a**INFN Sezione di Roma ^a, Sapienza Università di Roma ^b, Rome, Italy**L. Barone^{a,b}, F. Cavallari^a, M. Cipriani^{a,b}, N. Daci^a, D. Del Re^{a,b,15}, M. Diemoz^a, S. Gelli^{a,b}, E. Longo^{a,b}, F. Margaroli^{a,b}, B. Marzocchi^{a,b}, P. Meridiani^a, G. Organtini^{a,b}, R. Paramatti^{a,b}, F. Preiato^{a,b}, S. Rahatlou^{a,b}, C. Rovelli^a, F. Santanastasio^{a,b}**INFN Sezione di Torino ^a, Università di Torino ^b, Torino, Italy, Università del Piemonte Orientale ^c, Novara, Italy**N. Amapane^{a,b}, R. Arcidiacono^{a,c,15}, S. Argiro^{a,b}, M. Arneodo^{a,c}, N. Bartosik^a, R. Bellan^{a,b}, C. Biino^a, N. Cartiglia^a, F. Cenna^{a,b}, M. Costa^{a,b}, R. Covarelli^{a,b}, A. Degano^{a,b}, N. Demaria^a, B. Kiani^{a,b}, C. Mariotti^a, S. Maselli^a, E. Migliore^{a,b}, V. Monaco^{a,b}, E. Monteil^{a,b}, M. Monteno^a, M.M. Obertino^{a,b}, L. Pacher^{a,b}, N. Pastrone^a, M. Pelliccioni^a, G.L. Pinna Angioni^{a,b}, F. Ravera^{a,b}, A. Romero^{a,b}, M. Ruspa^{a,c}, R. Sacchi^{a,b}, K. Shchelina^{a,b}, V. Sola^a, A. Solano^{a,b}, A. Staiano^a, P. Traczyk^{a,b}**INFN Sezione di Trieste ^a, Università di Trieste ^b, Trieste, Italy**S. Belforte^a, M. Casarsa^a, F. Cossutti^a, G. Della Ricca^{a,b}, A. Zanetti^a

Kyungpook National University, Daegu, Korea

D.H. Kim, G.N. Kim, M.S. Kim, J. Lee, S. Lee, S.W. Lee, Y.D. Oh, S. Sekmen, D.C. Son, Y.C. Yang

Chonbuk National University, Jeonju, Korea

A. Lee

Chonnam National University, Institute for Universe and Elementary Particles, Kwangju, Korea

H. Kim, D.H. Moon, G. Oh

Hanyang University, Seoul, Korea

J.A. Brochero Cifuentes, J. Goh, T.J. Kim

Korea University, Seoul, Korea

S. Cho, S. Choi, Y. Go, D. Gyun, S. Ha, B. Hong, Y. Jo, Y. Kim, K. Lee, K.S. Lee, S. Lee, J. Lim, S.K. Park, Y. Roh

Seoul National University, Seoul, Korea

J. Almond, J. Kim, J.S. Kim, H. Lee, K. Lee, K. Nam, S.B. Oh, B.C. Radburn-Smith, S.h. Seo, U.K. Yang, H.D. Yoo, G.B. Yu

University of Seoul, Seoul, Korea

M. Choi, H. Kim, J.H. Kim, J.S.H. Lee, I.C. Park, G. Ryu

Sungkyunkwan University, Suwon, Korea

Y. Choi, C. Hwang, J. Lee, I. Yu

Vilnius University, Vilnius, Lithuania

V. Dudenas, A. Juodagalvis, J. Vaitkus

National Centre for Particle Physics, Universiti Malaya, Kuala Lumpur, Malaysia

I. Ahmed, Z.A. Ibrahim, M.A.B. Md Ali³², F. Mohamad Idris³³, W.A.T. Wan Abdullah, M.N. Yusli, Z. Zolkapli

Centro de Investigacion y de Estudios Avanzados del IPN, Mexico City, Mexico

H. Castilla-Valdez, E. De La Cruz-Burelo, I. Heredia-De La Cruz³⁴, R. Lopez-Fernandez, J. Mejia Guisao, A. Sanchez-Hernandez

Universidad Iberoamericana, Mexico City, Mexico

S. Carrillo Moreno, C. Oropeza Barrera, F. Vazquez Valencia

Benemerita Universidad Autonoma de Puebla, Puebla, Mexico

I. Pedraza, H.A. Salazar Ibarguen, C. Uribe Estrada

Universidad Autónoma de San Luis Potosí, San Luis Potosí, Mexico

A. Morelos Pineda

University of Auckland, Auckland, New Zealand

D. Krofcheck

University of Canterbury, Christchurch, New Zealand

P.H. Butler

National Centre for Physics, Quaid-I-Azam University, Islamabad, Pakistan

A. Ahmad, M. Ahmad, Q. Hassan, H.R. Hoorani, A. Saddique, M.A. Shah, M. Shoaib, M. Waqas

National Centre for Nuclear Research, Swierk, Poland

H. Bialkowska, M. Bluj, B. Boimska, T. Frueboes, M. Górski, M. Kazana, K. Nawrocki, K. Romanowska-Rybinska, M. Szleper, P. Zalewski

Institute of Experimental Physics, Faculty of Physics, University of Warsaw, Warsaw, Poland

K. Bunkowski, A. Byszuk³⁵, K. Doroba, A. Kalinowski, M. Konecki, J. Krolikowski, M. Misiura, M. Olszewski, A. Pyskir, M. Walczak

Laboratório de Instrumentação e Física Experimental de Partículas, Lisboa, Portugal

P. Bargassa, C. Beirão Da Cruz E Silva, B. Calpas, A. Di Francesco, P. Faccioli, M. Gallinaro, J. Hollar, N. Leonardo, L. Lloret Iglesias, M.V. Nemallapudi, J. Seixas, O. Toldaiev, D. Vadrucio, J. Varela

Joint Institute for Nuclear Research, Dubna, Russia

S. Afanasiev, P. Bunin, M. Gavrilenko, I. Golutvin, I. Gorbunov, A. Kamenev, V. Karjavin, A. Lanev, A. Malakhov, V. Matveev^{36,37}, V. Palichik, V. Perelygin, S. Shmatov, S. Shulha, N. Skatchkov, V. Smirnov, N. Voytishin, A. Zarubin

Petersburg Nuclear Physics Institute, Gatchina (St. Petersburg), Russia

Y. Ivanov, V. Kim³⁸, E. Kuznetsova³⁹, P. Levchenko, V. Murzin, V. Oreshkin, I. Smirnov, V. Sulimov, L. Uvarov, S. Vavilov, A. Vorobyev

Institute for Nuclear Research, Moscow, Russia

Yu. Andreev, A. Dermenev, S. Gninenko, N. Golubev, A. Karneyeu, M. Kirsanov, N. Krasnikov, A. Pashenkov, D. Tlisov, A. Toropin

Institute for Theoretical and Experimental Physics, Moscow, Russia

V. Epshteyn, V. Gavrillov, N. Lychkovskaya, V. Popov, I. Pozdnyakov, G. Safronov, A. Spiridonov, A. Steppenov, M. Toms, E. Vlasov, A. Zhokin

Moscow Institute of Physics and Technology, Moscow, Russia

T. Aushev, A. Bylinkin³⁷

National Research Nuclear University 'Moscow Engineering Physics Institute' (MEPhI), Moscow, Russia

M. Chadeeva⁴⁰, E. Popova, V. Rusinov

P.N. Lebedev Physical Institute, Moscow, Russia

V. Andreev, M. Azarkin³⁷, I. Dremin³⁷, M. Kirakosyan, A. Terkulov

Skobeltsyn Institute of Nuclear Physics, Lomonosov Moscow State University, Moscow, Russia

A. Baskakov, A. Belyaev, E. Boos, A. Demiyanov, A. Ershov, A. Gribushin, O. Kodolova, V. Korotkikh, I. Lokhtin, I. Miagkov, S. Obraztsov, S. Petrushanko, V. Savrin, A. Snigirev, I. Vardanyan

Novosibirsk State University (NSU), Novosibirsk, Russia

V. Blinov⁴¹, Y. Skovpen⁴¹, D. Shtol⁴¹

State Research Center of Russian Federation, Institute for High Energy Physics, Protvino, Russia

I. Azhgirey, I. Bayshev, S. Bitioukov, D. Elumakhov, V. Kachanov, A. Kalinin, D. Konstantinov, V. Krychkin, V. Petrov, R. Ryutin, A. Sobol, S. Troshin, N. Tyurin, A. Uzunian, A. Volkov

University of Belgrade, Faculty of Physics and Vinca Institute of Nuclear Sciences, Belgrade, Serbia

P. Adzic⁴², P. Cirkovic, D. Devetak, M. Dordevic, J. Milosevic, V. Rekovic

Centro de Investigaciones Energéticas Medioambientales y Tecnológicas (CIEMAT), Madrid, Spain

J. Alcaraz Maestre, M. Barrio Luna, M. Cerrada, N. Colino, B. De La Cruz, A. Delgado Peris, A. Escalante Del Valle, C. Fernandez Bedoya, J.P. Fernández Ramos, J. Flix, M.C. Fouz, P. Garcia-Abia, O. Gonzalez Lopez, S. Goy Lopez, J.M. Hernandez, M.I. Josa, A. Pérez-Calero Yzquierdo, J. Puerta Pelayo, A. Quintario Olmeda, I. Redondo, L. Romero, M.S. Soares, A. Álvarez Fernández

Universidad Autónoma de Madrid, Madrid, Spain

J.F. de Trocóniz, M. Missiroli, D. Moran

Universidad de Oviedo, Oviedo, Spain

J. Cuevas, C. Erice, J. Fernandez Menendez, I. Gonzalez Caballero, J.R. González Fernández, E. Palencia Cortezon, S. Sanchez Cruz, I. Suárez Andrés, P. Vischia, J.M. Vizán Garcia

Instituto de Física de Cantabria (IFCA), CSIC-Universidad de Cantabria, Santander, Spain

I.J. Cabrillo, A. Calderon, B. Chazin Quero, E. Curras, M. Fernandez, J. Garcia-Ferrero, G. Gomez, A. Lopez Virto, J. Marco, C. Martinez Rivero, P. Martinez Ruiz del Arbol, F. Matorras, J. Piedra Gomez, T. Rodrigo, A. Ruiz-Jimeno, L. Scodellaro, N. Trevisani, I. Vila, R. Vilar Cortabitarte

CERN, European Organization for Nuclear Research, Geneva, Switzerland

D. Abbaneo, E. Auffray, P. Baillon, A.H. Ball, D. Barney, M. Bianco, P. Bloch, A. Bocci, C. Botta, T. Camporesi, R. Castello, M. Cepeda, G. Cerminara, E. Chapon, Y. Chen, D. d'Enterria, A. Dabrowski, V. Daponte, A. David, M. De Gruttola, A. De Roeck, E. Di Marco⁴³, M. Dobson, B. Dorney, T. du Pree, M. Dünser, N. Dupont, A. Elliott-Peisert, P. Everaerts, G. Franzoni, J. Fulcher, W. Funk, D. Gigi, K. Gill, F. Glege, D. Gulhan, S. Gundacker, M. Guthoff, P. Harris, J. Hegeman, V. Innocente, P. Janot, O. Karacheban¹⁸, J. Kieseler, H. Kirschenmann, V. Knünz, A. Kornmayer¹⁵, M.J. Kortelainen, M. Krammer¹, C. Lange, P. Lecoq, C. Lourenço, M.T. Lucchini, L. Malgeri, M. Mannelli, A. Martelli, F. Meijers, J.A. Merlin, S. Mersi, E. Meschi, P. Milenovic⁴⁴, F. Moortgat, M. Mulders, H. Neugebauer, S. Orfanelli, L. Orsini, L. Pape, E. Perez, M. Peruzzi, A. Petrilli, G. Petrucciani, A. Pfeiffer, M. Pierini, A. Racz, T. Reis, G. Rolandi⁴⁵, M. Rovere, H. Sakulin, C. Schäfer, C. Schwick, M. Seidel, M. Selvaggi, A. Sharma, P. Silva, P. Sphicas⁴⁶, J. Steggemann, M. Stoye, M. Tosi, D. Treille, A. Triossi, A. Tsirou, V. Veckalns⁴⁷, G.I. Veres²⁰, M. Verweij, N. Wardle, W.D. Zeuner

Paul Scherrer Institut, Villigen, Switzerland

W. Bertl[†], K. Deiters, W. Erdmann, R. Horisberger, Q. Ingram, H.C. Kaestli, D. Kotlinski, U. Langenegger, T. Rohe, S.A. Wiederkehr

Institute for Particle Physics, ETH Zurich, Zurich, Switzerland

F. Bachmair, L. Bäni, P. Berger, L. Bianchini, B. Casal, G. Dissertori, M. Dittmar, M. Donegà, C. Grab, C. Heidegger, D. Hits, J. Hoss, G. Kasieczka, T. Klijsma, W. Lustermann, B. Mangano, M. Marionneau, M.T. Meinhard, D. Meister, F. Micheli, P. Musella, F. Nessi-Tedaldi, F. Pandolfi, J. Pata, F. Pauss, G. Perrin, L. Perrozzi, M. Quittnat, M. Rossini, M. Schönenberger, L. Shchutska, A. Starodumov⁴⁸, V.R. Tavolaro, K. Theofilatos, M.L. Vesterbacka Olsson, R. Wallny, A. Zagozdinska³⁵, D.H. Zhu

Universität Zürich, Zurich, Switzerland

T.K. Aarrestad, C. Amsler⁴⁹, L. Caminada, M.F. Canelli, A. De Cosa, S. Donato, C. Galloni, A. Hinzmann, T. Hreus, B. Kilminster, J. Ngadiuba, D. Pinna, G. Rauco, P. Robmann, D. Salerno, C. Seitz, A. Zucchetta

National Central University, Chung-Li, Taiwan

V. Candelise, T.H. Doan, Sh. Jain, R. Khurana, M. Konyushikhin, C.M. Kuo, W. Lin, A. Pozdnyakov, S.S. Yu

National Taiwan University (NTU), Taipei, Taiwan

Arun Kumar, P. Chang, Y. Chao, K.F. Chen, P.H. Chen, F. Fiori, W.-S. Hou, Y. Hsiung, Y.F. Liu, R.-S. Lu, M. Miñano Moya, E. Paganis, A. Psallidas, J.f. Tsai

Chulalongkorn University, Faculty of Science, Department of Physics, Bangkok, Thailand

B. Asavapibhop, K. Kovitanggoon, G. Singh, N. Srimanobhas

Çukurova University, Physics Department, Science and Art Faculty, Adana, Turkey

A. Adiguzel⁵⁰, M.N. Bakirci⁵¹, F. Boran, S. Cerci⁵², S. Damarseckin, Z.S. Demiroglu, C. Dozen, I. Dumanoglu, S. Girgis, G. Gokbulut, Y. Guler, I. Hos⁵³, E.E. Kangal⁵⁴, O. Kara, A. Kayis Topaksu, U. Kiminsu, M. Oglakci, G. Onengut⁵⁵, K. Ozdemir⁵⁶, B. Tali⁵², S. Turkcapar, I.S. Zorbakir, C. Zorbilmez

Middle East Technical University, Physics Department, Ankara, Turkey

B. Bilin, G. Karapinar⁵⁷, K. Ocalan⁵⁸, M. Yalvac, M. Zeyrek

Bogazici University, Istanbul, Turkey

E. Gülmez, M. Kaya⁵⁹, O. Kaya⁶⁰, S. Tekten, E.A. Yetkin⁶¹

Istanbul Technical University, Istanbul, Turkey

M.N. Agaras, S. Atay, A. Cakir, K. Cankocak

Institute for Scintillation Materials of National Academy of Science of Ukraine, Kharkov, Ukraine

B. Grynyov

National Scientific Center, Kharkov Institute of Physics and Technology, Kharkov, Ukraine

L. Levchuk, P. Sorokin

University of Bristol, Bristol, United Kingdom

R. Aggleton, F. Ball, L. Beck, J.J. Brooke, D. Burns, E. Clement, D. Cussans, H. Flacher, J. Goldstein, M. Grimes, G.P. Heath, H.F. Heath, J. Jacob, L. Kreczko, C. Lucas, D.M. Newbold⁶², S. Paramesvaran, A. Poll, T. Sakuma, S. Seif El Nasr-storey, D. Smith, V.J. Smith

Rutherford Appleton Laboratory, Didcot, United Kingdom

A. Belyaev⁶³, C. Brew, R.M. Brown, L. Calligaris, D. Cieri, D.J.A. Cockerill, J.A. Coughlan, K. Harder, S. Harper, E. Olaiya, D. Petyt, C.H. Shepherd-Themistocleous, A. Thea, I.R. Tomalin, T. Williams

Imperial College, London, United Kingdom

M. Baber, R. Bainbridge, S. Breeze, O. Buchmuller, A. Bundock, S. Casasso, M. Citron, D. Colling, L. Corpe, P. Dauncey, G. Davies, A. De Wit, M. Della Negra, R. Di Maria, P. Dunne, A. Elwood, D. Futyan, Y. Haddad, G. Hall, G. Iles, T. James, R. Lane, C. Laner, L. Lyons, A.-M. Magnan, S. Malik, L. Mastrolorenzo, T. Matsushita, J. Nash, A. Nikitenko⁴⁸, J. Pela, M. Pesaresi, D.M. Raymond, A. Richards, A. Rose, E. Scott, C. Seez, A. Shtipliyski, S. Summers, A. Tapper, K. Uchida, M. Vazquez Acosta⁶⁴, T. Virdee¹⁵, D. Winterbottom, J. Wright, S.C. Zenz

Brunel University, Uxbridge, United Kingdom

J.E. Cole, P.R. Hobson, A. Khan, P. Kyberd, I.D. Reid, P. Symonds, L. Teodorescu, M. Turner

Baylor University, Waco, USA

A. Borzou, K. Call, J. Dittmann, K. Hatakeyama, H. Liu, N. Pastika

Catholic University of America, Washington DC, USA

R. Bartek, A. Dominguez

The University of Alabama, Tuscaloosa, USA

A. Buccilli, S.I. Cooper, C. Henderson, P. Rumerio, C. West

Boston University, Boston, USA

D. Arcaro, A. Avetisyan, T. Bose, D. Gastler, D. Rankin, C. Richardson, J. Rohlf, L. Sulak, D. Zou

Brown University, Providence, USA

G. Benelli, D. Cutts, A. Garabedian, J. Hakala, U. Heintz, J.M. Hogan, K.H.M. Kwok, E. Laird, G. Landsberg, Z. Mao, M. Narain, J. Pazzini, S. Piperov, S. Sagir, R. Syarif, D. Yu

University of California, Davis, Davis, USA

R. Band, C. Brainerd, D. Burns, M. Calderon De La Barca Sanchez, M. Chertok, J. Conway, R. Conway, P.T. Cox, R. Erbacher, C. Flores, G. Funk, M. Gardner, W. Ko, R. Lander, C. Mclean, M. Mulhearn, D. Pellett, J. Pilot, S. Shalhout, M. Shi, J. Smith, M. Squires, D. Stolp, K. Tos, M. Tripathi, Z. Wang

University of California, Los Angeles, USA

M. Bachtis, C. Bravo, R. Cousins, A. Dasgupta, A. Florent, J. Hauser, M. Ignatenko, N. Mccoll, D. Saltzberg, C. Schnaible, V. Valuev

University of California, Riverside, Riverside, USA

E. Bouvier, K. Burt, R. Clare, J. Ellison, J.W. Gary, S.M.A. Ghiasi Shirazi, G. Hanson, J. Heilman, P. Jandir, E. Kennedy, F. Lacroix, O.R. Long, M. Olmedo Negrete, M.I. Paneva, A. Shrinivas, W. Si, H. Wei, S. Wimpenny, B. R. Yates

University of California, San Diego, La Jolla, USA

J.G. Branson, G.B. Cerati, S. Cittolin, M. Derdzinski, R. Gerosa, B. Hashemi, A. Holzner, D. Klein, G. Kole, V. Krutelyov, J. Letts, I. Macneill, M. Masciovecchio, D. Olivito, S. Padhi, M. Pieri, M. Sani, V. Sharma, S. Simon, M. Tadel, A. Vartak, S. Wasserbaech⁶⁵, J. Wood, F. Würthwein, A. Yagil, G. Zevi Della Porta

University of California, Santa Barbara - Department of Physics, Santa Barbara, USA

N. Amin, R. Bhandari, J. Bradmiller-Feld, C. Campagnari, A. Dishaw, V. Dutta, M. Franco Sevilla, C. George, F. Golf, L. Gouskos, J. Gran, R. Heller, J. Incandela, S.D. Mullin, A. Ovcharova, H. Qu, J. Richman, D. Stuart, I. Suarez, J. Yoo

California Institute of Technology, Pasadena, USA

D. Anderson, J. Bendavid, A. Bornheim, J.M. Lawhorn, H.B. Newman, T. Nguyen, C. Pena, M. Spiropulu, J.R. Vlimant, S. Xie, Z. Zhang, R.Y. Zhu

Carnegie Mellon University, Pittsburgh, USA

M.B. Andrews, T. Ferguson, T. Mudholkar, M. Paulini, J. Russ, M. Sun, H. Vogel, I. Vorobiev, M. Weinberg

University of Colorado Boulder, Boulder, USA

J.P. Cumalat, W.T. Ford, F. Jensen, A. Johnson, M. Krohn, S. Leontsinis, T. Mulholland, K. Stenson, S.R. Wagner

Cornell University, Ithaca, USA

J. Alexander, J. Chaves, J. Chu, S. Dittmer, K. McDermott, N. Mirman, J.R. Patterson, A. Rinkevicius, A. Ryd, L. Skinnari, L. Soffi, S.M. Tan, Z. Tao, J. Thom, J. Tucker, P. Wittich, M. Zientek

Fermi National Accelerator Laboratory, Batavia, USA

S. Abdullin, M. Albrow, G. Apollinari, A. Apresyan, A. Apyan, S. Banerjee, L.A.T. Bauerdick, A. Beretvas, J. Berryhill, P.C. Bhat, G. Bolla, K. Burkett, J.N. Butler, A. Canepa, H.W.K. Cheung, F. Chlebana, M. Cremonesi, J. Duarte, V.D. Elvira, J. Freeman, Z. Gecse, E. Gottschalk, L. Gray, D. Green, S. Grünendahl, O. Gutsche, R.M. Harris, S. Hasegawa, J. Hirschauer, Z. Hu, B. Jayatilaka, S. Jindariani, M. Johnson, U. Joshi, B. Klima, B. Kreis, S. Lammel, D. Lincoln, R. Lipton, M. Liu, T. Liu, R. Lopes De Sá, J. Lykken, K. Maeshima, N. Magini, J.M. Marraffino, S. Maruyama, D. Mason, P. McBride, P. Merkel, S. Mrenna, S. Nahn, V. O'Dell, K. Pedro, O. Prokofyev, G. Rakness, L. Ristori, B. Schneider, E. Sexton-Kennedy, A. Soha, W.J. Spalding, L. Spiegel, S. Stoynev, J. Strait, N. Strobbe, L. Taylor, S. Tkaczyk, N.V. Tran, L. Uplegger, E.W. Vaandering, C. Vernieri, M. Verzocchi, R. Vidal, M. Wang, H.A. Weber, A. Whitbeck

University of Florida, Gainesville, USA

D. Acosta, P. Avery, P. Bortignon, A. Brinkerhoff, A. Carnes, M. Carver, D. Curry, S. Das, R.D. Field, I.K. Furic, J. Konigsberg, A. Korytov, K. Kotov, P. Ma, K. Matchev, H. Mei, G. Mitselmakher, D. Rank, D. Sperka, N. Terentyev, L. Thomas, J. Wang, S. Wang, J. Yelton

Florida International University, Miami, USA

Y.R. Joshi, S. Linn, P. Markowitz, G. Martinez, J.L. Rodriguez

Florida State University, Tallahassee, USA

A. Ackert, T. Adams, A. Askew, S. Hagopian, V. Hagopian, K.F. Johnson, T. Kolberg, T. Perry, H. Prosper, A. Santra, R. Yohay

Florida Institute of Technology, Melbourne, USA

M.M. Baarmand, V. Bhopatkar, S. Colafranceschi, M. Hohlmann, D. Noonan, T. Roy, F. Yumiceva

University of Illinois at Chicago (UIC), Chicago, USA

M.R. Adams, L. Apanasevich, D. Berry, R.R. Betts, R. Cavanaugh, X. Chen, O. Evdokimov, C.E. Gerber, D.A. Hangal, D.J. Hofman, K. Jung, J. Kamin, I.D. Sandoval Gonzalez, M.B. Tonjes, H. Trauger, N. Varelas, H. Wang, Z. Wu, J. Zhang

The University of Iowa, Iowa City, USA

B. Bilki⁶⁶, W. Clarida, K. Dilsiz⁶⁷, S. Durgut, R.P. Gandrajula, M. Haytmyradov, V. Khristenko, J.-P. Merlo, H. Mermerkaya⁶⁸, A. Mestvirishvili, A. Moeller, J. Nachtman, H. Ogul⁶⁹, Y. Onel, F. Ozok⁷⁰, A. Penzo, C. Snyder, E. Tiras, J. Wetzel, K. Yi

Johns Hopkins University, Baltimore, USA

B. Blumenfeld, A. Cocoros, N. Eminizer, D. Fehling, L. Feng, A.V. Gritsan, P. Maksimovic, J. Roskes, U. Sarica, M. Swartz, M. Xiao, C. You

The University of Kansas, Lawrence, USA

A. Al-bataineh, P. Baringer, A. Bean, S. Boren, J. Bowen, J. Castle, S. Khalil, A. Kropivnitskaya, D. Majumder, W. Mcbrayer, M. Murray, C. Royon, S. Sanders, E. Schmitz, R. Stringer, J.D. Tapia Takaki, Q. Wang

Kansas State University, Manhattan, USA

A. Ivanov, K. Kaadze, Y. Maravin, A. Mohammadi, L.K. Saini, N. Skhirtladze, S. Toda

Lawrence Livermore National Laboratory, Livermore, USA

F. Rebassoo, D. Wright

University of Maryland, College Park, USA

C. Anelli, A. Baden, O. Baron, A. Belloni, B. Calvert, S.C. Eno, C. Ferraioli, N.J. Hadley, S. Jabeen, G.Y. Jeng, R.G. Kellogg, J. Kunkle, A.C. Mignerey, F. Ricci-Tam, Y.H. Shin, A. Skuja, S.C. Tonwar

Massachusetts Institute of Technology, Cambridge, USA

D. Abercrombie, B. Allen, V. Azzolini, R. Barbieri, A. Baty, R. Bi, S. Brandt, W. Busza, I.A. Cali, M. D'Alfonso, Z. Demiragli, G. Gomez Ceballos, M. Goncharov, D. Hsu, Y. Iiyama, G.M. Innocenti, M. Klute, D. Kovalskyi, Y.S. Lai, Y.-J. Lee, A. Levin, P.D. Luckey, B. Maier, A.C. Marini, C. Mcginn, C. Mironov, S. Narayanan, X. Niu, C. Paus, C. Roland, G. Roland, J. Salfeld-Nebgen, G.S.F. Stephans, K. Tatar, D. Velicanu, J. Wang, T.W. Wang, B. Wyslouch

University of Minnesota, Minneapolis, USA

A.C. Benvenuti, R.M. Chatterjee, A. Evans, P. Hansen, S. Kalafut, Y. Kubota, Z. Lesko, J. Mans, S. Nourbakhsh, N. Ruckstuhl, R. Rusack, J. Turkewitz

University of Mississippi, Oxford, USA

J.G. Acosta, S. Oliveros

University of Nebraska-Lincoln, Lincoln, USA

E. Avdeeva, K. Bloom, D.R. Claes, C. Fangmeier, R. Gonzalez Suarez, R. Kamalieddin, I. Kravchenko, J. Monroy, J.E. Siado, G.R. Snow, B. Stieger

State University of New York at Buffalo, Buffalo, USA

M. Alyari, J. Dolen, A. Godshalk, C. Harrington, I. Iashvili, D. Nguyen, A. Parker, S. Rappoccio, B. Roozbahani

Northeastern University, Boston, USA

G. Alverson, E. Barberis, A. Hortiangtham, A. Massironi, D.M. Morse, D. Nash, T. Orimoto, R. Teixeira De Lima, D. Trocino, R.-J. Wang, D. Wood

Northwestern University, Evanston, USA

S. Bhattacharya, O. Charaf, K.A. Hahn, N. Mucia, N. Odell, B. Pollack, M.H. Schmitt, K. Sung, M. Trovato, M. Velasco

University of Notre Dame, Notre Dame, USA

N. Dev, M. Hildreth, K. Hurtado Anampa, C. Jessop, D.J. Karmgard, N. Kellams, K. Lannon, N. Loukas, N. Marinelli, F. Meng, C. Mueller, Y. Musienko³⁶, M. Planer, A. Reinsvold, R. Ruchti, G. Smith, S. Taroni, M. Wayne, M. Wolf, A. Woodard

The Ohio State University, Columbus, USA

J. Alimena, L. Antonelli, B. Bylsma, L.S. Durkin, S. Flowers, B. Francis, A. Hart, C. Hill, W. Ji, B. Liu, W. Luo, D. Puigh, B.L. Winer, H.W. Wulsin

Princeton University, Princeton, USA

A. Benaglia, S. Cooperstein, O. Driga, P. Elmer, J. Hardenbrook, P. Hebda, D. Lange, J. Luo, D. Marlow, K. Mei, I. Ojalvo, J. Olsen, C. Palmer, P. Piroué, D. Stickland, A. Svyatkovskiy, C. Tully

University of Puerto Rico, Mayaguez, USA

S. Malik, S. Norberg

Purdue University, West Lafayette, USA

A. Barker, V.E. Barnes, S. Folgueras, L. Gutay, M.K. Jha, M. Jones, A.W. Jung, A. Khatiwada, D.H. Miller, N. Neumeister, J.F. Schulte, J. Sun, F. Wang, W. Xie

Purdue University Northwest, Hammond, USA

T. Cheng, N. Parashar, J. Stupak

Rice University, Houston, USA

A. Adair, B. Akgun, Z. Chen, K.M. Ecklund, F.J.M. Geurts, M. Guilbaud, W. Li, B. Michlin, M. Northup, B.P. Padley, J. Roberts, J. Rorie, Z. Tu, J. Zabel

University of Rochester, Rochester, USA

A. Bodek, P. de Barbaro, R. Demina, Y.t. Duh, T. Ferbel, M. Galanti, A. Garcia-Bellido, J. Han, O. Hindrichs, A. Khukhunaishvili, K.H. Lo, P. Tan, M. Verzetti

The Rockefeller University, New York, USA

R. Ciesielski, K. Goulianos, C. Mesropian

Rutgers, The State University of New Jersey, Piscataway, USA

A. Agapitos, J.P. Chou, Y. Gershtein, T.A. Gómez Espinosa, E. Halkiadakis, M. Heindl, E. Hughes, S. Kaplan, R. Kunnawalkam Elayavalli, S. Kyriacou, A. Lath, R. Montalvo, K. Nash, M. Osherson, H. Saka, S. Salur, S. Schnetzer, D. Sheffield, S. Somalwar, R. Stone, S. Thomas, P. Thomassen, M. Walker

University of Tennessee, Knoxville, USA

M. Foerster, J. Heideman, G. Riley, K. Rose, S. Spanier, K. Thapa

Texas A&M University, College Station, USA

O. Bouhali⁷¹, A. Castaneda Hernandez⁷¹, A. Celik, M. Dalchenko, M. De Mattia, A. Delgado, S. Dildick, R. Eusebi, J. Gilmore, T. Huang, T. Kamon⁷², R. Mueller, Y. Pakhotin, R. Patel, A. Perloff, L. Perniè, D. Rathjens, A. Safonov, A. Tatarinov, K.A. Ulmer

Texas Tech University, Lubbock, USA

N. Akchurin, J. Damgov, F. De Guio, P.R. Duderø, J. Faulkner, E. Gurpinar, S. Kunori, K. Lamichhane, S.W. Lee, T. Libeiro, T. Peltola, S. Undleeb, I. Volobouev, Z. Wang

Vanderbilt University, Nashville, USA

S. Greene, A. Gurrola, R. Janjam, W. Johns, C. Maguire, A. Melo, H. Ni, P. Sheldon, S. Tuo, J. Velkovska, Q. Xu

University of Virginia, Charlottesville, USA

M.W. Arenton, P. Barria, B. Cox, R. Hirosky, A. Ledovskoy, H. Li, C. Neu, T. Sinthuprasith, X. Sun, Y. Wang, E. Wolfe, F. Xia

Wayne State University, Detroit, USA

C. Clarke, R. Harr, P.E. Karchin, J. Sturdy, S. Zaleski

University of Wisconsin - Madison, Madison, WI, USA

J. Buchanan, C. Caillol, S. Dasu, L. Dodd, S. Duric, B. Gomber, M. Grothe, M. Herndon, A. Hervé, U. Hussain, P. Klabbers, A. Lanaro, A. Levine, K. Long, R. Loveless, G.A. Pierro, G. Polese, T. Ruggles, A. Savin, N. Smith, W.H. Smith, D. Taylor, N. Woods

†: Deceased

1: Also at Vienna University of Technology, Vienna, Austria

2: Also at State Key Laboratory of Nuclear Physics and Technology, Peking University, Beijing, China

- 3: Also at Universidade Estadual de Campinas, Campinas, Brazil
- 4: Also at Universidade Federal de Pelotas, Pelotas, Brazil
- 5: Also at Université Libre de Bruxelles, Bruxelles, Belgium
- 6: Also at Joint Institute for Nuclear Research, Dubna, Russia
- 7: Also at Helwan University, Cairo, Egypt
- 8: Now at Zewail City of Science and Technology, Zewail, Egypt
- 9: Now at Fayoum University, El-Fayoum, Egypt
- 10: Also at British University in Egypt, Cairo, Egypt
- 11: Now at Ain Shams University, Cairo, Egypt
- 12: Also at Université de Haute Alsace, Mulhouse, France
- 13: Also at Skobeltsyn Institute of Nuclear Physics, Lomonosov Moscow State University, Moscow, Russia
- 14: Also at Tbilisi State University, Tbilisi, Georgia
- 15: Also at CERN, European Organization for Nuclear Research, Geneva, Switzerland
- 16: Also at RWTH Aachen University, III. Physikalisches Institut A, Aachen, Germany
- 17: Also at University of Hamburg, Hamburg, Germany
- 18: Also at Brandenburg University of Technology, Cottbus, Germany
- 19: Also at Institute of Nuclear Research ATOMKI, Debrecen, Hungary
- 20: Also at MTA-ELTE Lendület CMS Particle and Nuclear Physics Group, Eötvös Loránd University, Budapest, Hungary
- 21: Also at Institute of Physics, University of Debrecen, Debrecen, Hungary
- 22: Also at Indian Institute of Technology Bhubaneswar, Bhubaneswar, India
- 23: Also at Institute of Physics, Bhubaneswar, India
- 24: Also at University of Visva-Bharati, Santiniketan, India
- 25: Also at University of Ruhuna, Matara, Sri Lanka
- 26: Also at Isfahan University of Technology, Isfahan, Iran
- 27: Also at Yazd University, Yazd, Iran
- 28: Also at Plasma Physics Research Center, Science and Research Branch, Islamic Azad University, Tehran, Iran
- 29: Also at Università degli Studi di Siena, Siena, Italy
- 30: Also at INFN Sezione di Milano-Bicocca; Università di Milano-Bicocca, Milano, Italy
- 31: Also at Purdue University, West Lafayette, USA
- 32: Also at International Islamic University of Malaysia, Kuala Lumpur, Malaysia
- 33: Also at Malaysian Nuclear Agency, MOSTI, Kajang, Malaysia
- 34: Also at Consejo Nacional de Ciencia y Tecnología, Mexico city, Mexico
- 35: Also at Warsaw University of Technology, Institute of Electronic Systems, Warsaw, Poland
- 36: Also at Institute for Nuclear Research, Moscow, Russia
- 37: Now at National Research Nuclear University 'Moscow Engineering Physics Institute' (MEPhI), Moscow, Russia
- 38: Also at St. Petersburg State Polytechnical University, St. Petersburg, Russia
- 39: Also at University of Florida, Gainesville, USA
- 40: Also at P.N. Lebedev Physical Institute, Moscow, Russia
- 41: Also at Budker Institute of Nuclear Physics, Novosibirsk, Russia
- 42: Also at Faculty of Physics, University of Belgrade, Belgrade, Serbia
- 43: Also at INFN Sezione di Roma; Sapienza Università di Roma, Rome, Italy
- 44: Also at University of Belgrade, Faculty of Physics and Vinca Institute of Nuclear Sciences, Belgrade, Serbia
- 45: Also at Scuola Normale e Sezione dell'INFN, Pisa, Italy
- 46: Also at National and Kapodistrian University of Athens, Athens, Greece

- 47: Also at Riga Technical University, Riga, Latvia
- 48: Also at Institute for Theoretical and Experimental Physics, Moscow, Russia
- 49: Also at Albert Einstein Center for Fundamental Physics, Bern, Switzerland
- 50: Also at Istanbul University, Faculty of Science, Istanbul, Turkey
- 51: Also at Gaziosmanpasa University, Tokat, Turkey
- 52: Also at Adiyaman University, Adiyaman, Turkey
- 53: Also at Istanbul Aydin University, Istanbul, Turkey
- 54: Also at Mersin University, Mersin, Turkey
- 55: Also at Cag University, Mersin, Turkey
- 56: Also at Piri Reis University, Istanbul, Turkey
- 57: Also at Izmir Institute of Technology, Izmir, Turkey
- 58: Also at Necmettin Erbakan University, Konya, Turkey
- 59: Also at Marmara University, Istanbul, Turkey
- 60: Also at Kafkas University, Kars, Turkey
- 61: Also at Istanbul Bilgi University, Istanbul, Turkey
- 62: Also at Rutherford Appleton Laboratory, Didcot, United Kingdom
- 63: Also at School of Physics and Astronomy, University of Southampton, Southampton, United Kingdom
- 64: Also at Instituto de Astrofísica de Canarias, La Laguna, Spain
- 65: Also at Utah Valley University, Orem, USA
- 66: Also at Beykent University, Istanbul, Turkey
- 67: Also at Bingol University, Bingol, Turkey
- 68: Also at Erzincan University, Erzincan, Turkey
- 69: Also at Sinop University, Sinop, Turkey
- 70: Also at Mimar Sinan University, Istanbul, Istanbul, Turkey
- 71: Also at Texas A&M University at Qatar, Doha, Qatar
- 72: Also at Kyungpook National University, Daegu, Korea